Master Thesis in Geosciences

Angola margin: regional tectonic evolution based on integrated analysis of seismic reflection and potential field data and modelling

by

Rauza Nurullina

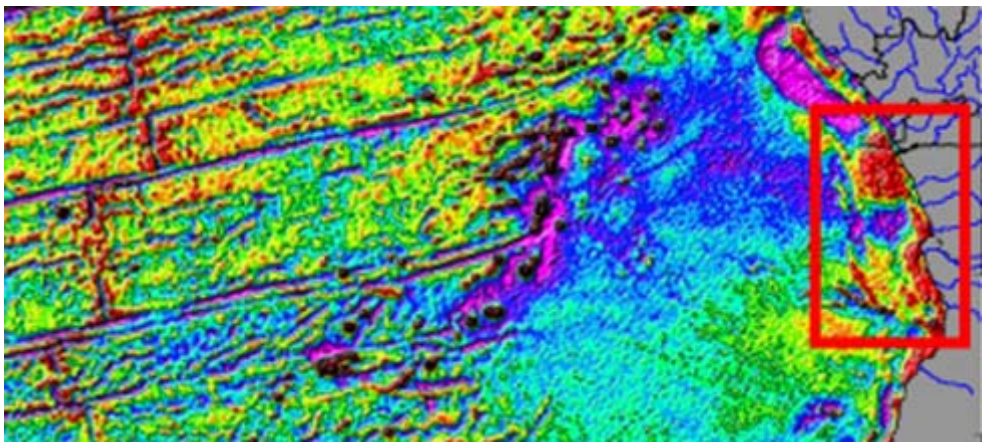

UNIVERSITY OF OSLO

FACULTY OF MATHEMATICS AND NATURAL SCIENCES

Angola margin: regional tectonic evolution based on integrated analysis of seismic reflection and potential field data and modelling

by

Rauza Nurullina

Master Thesis in Geosciences

Discipline: Petroleum Geology and Geophysics

Department of Geosciences

Faculty of Mathematics and Natural Sciences

UNIVERSITY OF OSLO

[June 2006]

Tutor(s): Prof. Jan Inge Faleide and Assoc. Prof. Filippos Tsikalas, UiO

This work is published digitally through DUO – Digitale Utgivelser ved UiO

http://www.duo.uio.no

It is also catalogued in BIBSYS (http://www.bibsys.no/english)

CONTENTS

PREFACE

This paper represents a Master Thesis finalising studies at University of Oslo, Master of Science program “Petroleum Geology and Geophysics” (2005 – 2006). The author thanks the teachers of the Department of Geosciences, University of Oslo. It is a pleasure to acknowledge a great respect and gratefulness to the supervisors of this work, Prof. Jan Inge Faleide and Assoc. prof. Filippos Tsikalas. Their patience, stimulating discussions and critical review of the manuscript provided tremendous support for this work. The author is glad to express special thanks to a personal friend Klaus Wiman who made these studies possible.

1. INTRODUCTION

Present day plate tectonic setting of the South Atlantic evolved via a complex history. There was significant extension from about 210 Ma (end Triassic) until the South Atlantic opened at about 130 Ma (Early Cretaceous). Since final breakup of Gondwana offshore West Africa has developed as a passive margin. A range of competing processes influenced the continental margin evolution. Such processes as extension accompanied by faulting and block rotation, thermal subsidence, continental uplift, magmatism, gravity driven salt tectonics and sediment progradation have produced the present day structure of the margin. Thick sedimentary successions, magmatism and salt layers have challenged the studies of the margins.

The study area of this work is part of the West Africa continental margin - offshore Angola (Fig. 1.1). Despite the large amount of data acquired, the geometries of subsalt sedimentary layers and lower crustal structure offshore Angola remain much debated due to masking effect of the Aptian salt layer and low seismic resolution at large depths. The robust methodology integrating the analysis of seismic reflection and potential field data with the gravity modelling is suggested in this work as a possible approach for tackling the problems in passive margin studies.

The data on which this work is based consist of published seismic transects from Marton et al. (2000) and publicly available data sets for the world's oceans, such as high resolution ship-track measurements, gridded satellite-radar-altimeter free-air gravity anomaly data and gridded bathymetry data, and a digital total sediment thickness database for the world's oceans and marginal seas.

The present work is an attempt to provide the geometry of the crustal structure of the Angola margin on the basis of integrated analysis of seismic reflection and potential field data and gravity modelling. The main objectives of the work were to define the crustal structure of the Angola margin, to delineate the continent-ocean boundary/transition (COB/COT), refine the margin segmentation due to a number of transfer zones, study magmatism along the margin, refine the plate tectonics, rift and shear structure, to study symmetry/asymmetry of the conjugate part of the Brazilian continental margin (Fig. 1.1). The elements of the margin architecture are together important for understanding of the process of margin formation and therefore essential for exploration and evaluation of hydrocarbon potential.

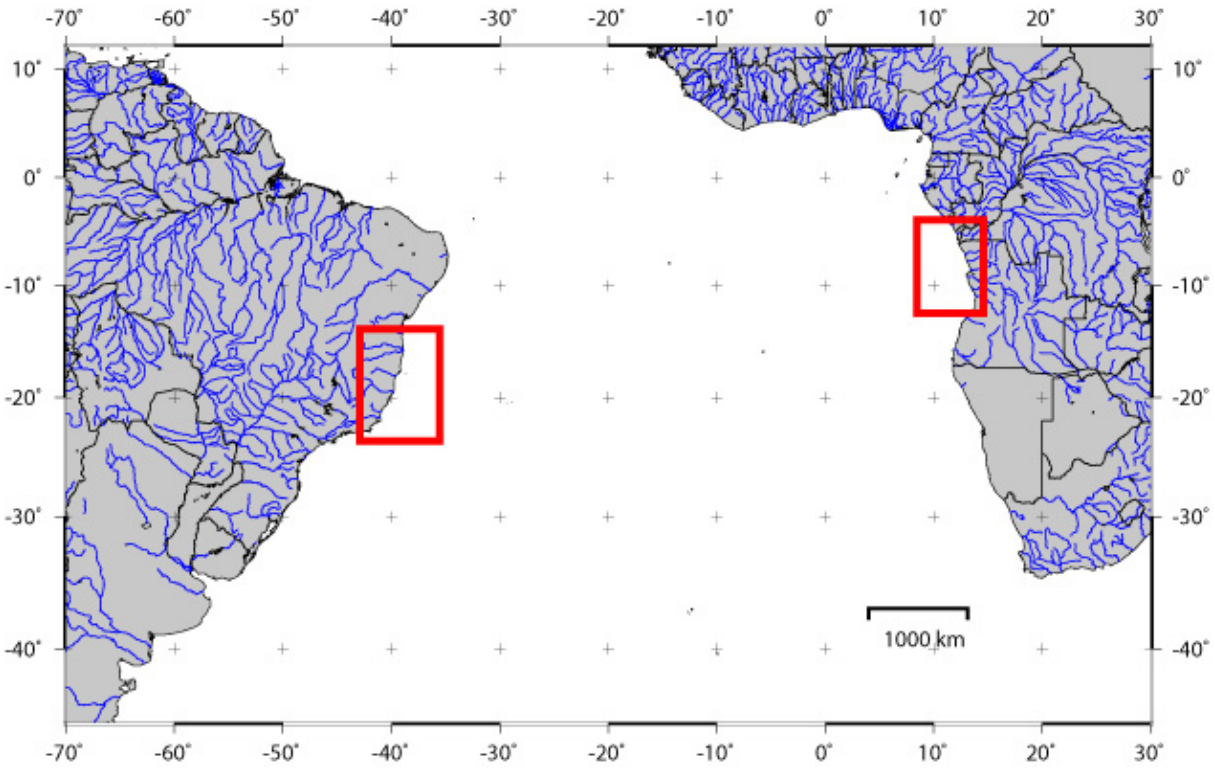

Figure 1.1 The South Atlantic. The study area of this work and the conjugate part of the Brazilian margin are highlighted with red boxes.

2. GEOLOGICAL FRAMEWORK

2.1 Plate tectonic evolution of the South Atlantic

The modern South Atlantic margins started their evolution as part of a continental rift system that developed in the southern parts of the Gondwana super-continent at the Jurassic-Cretaceous transition (Fig. 2.1) (Gjelberg & Valle, 2003).

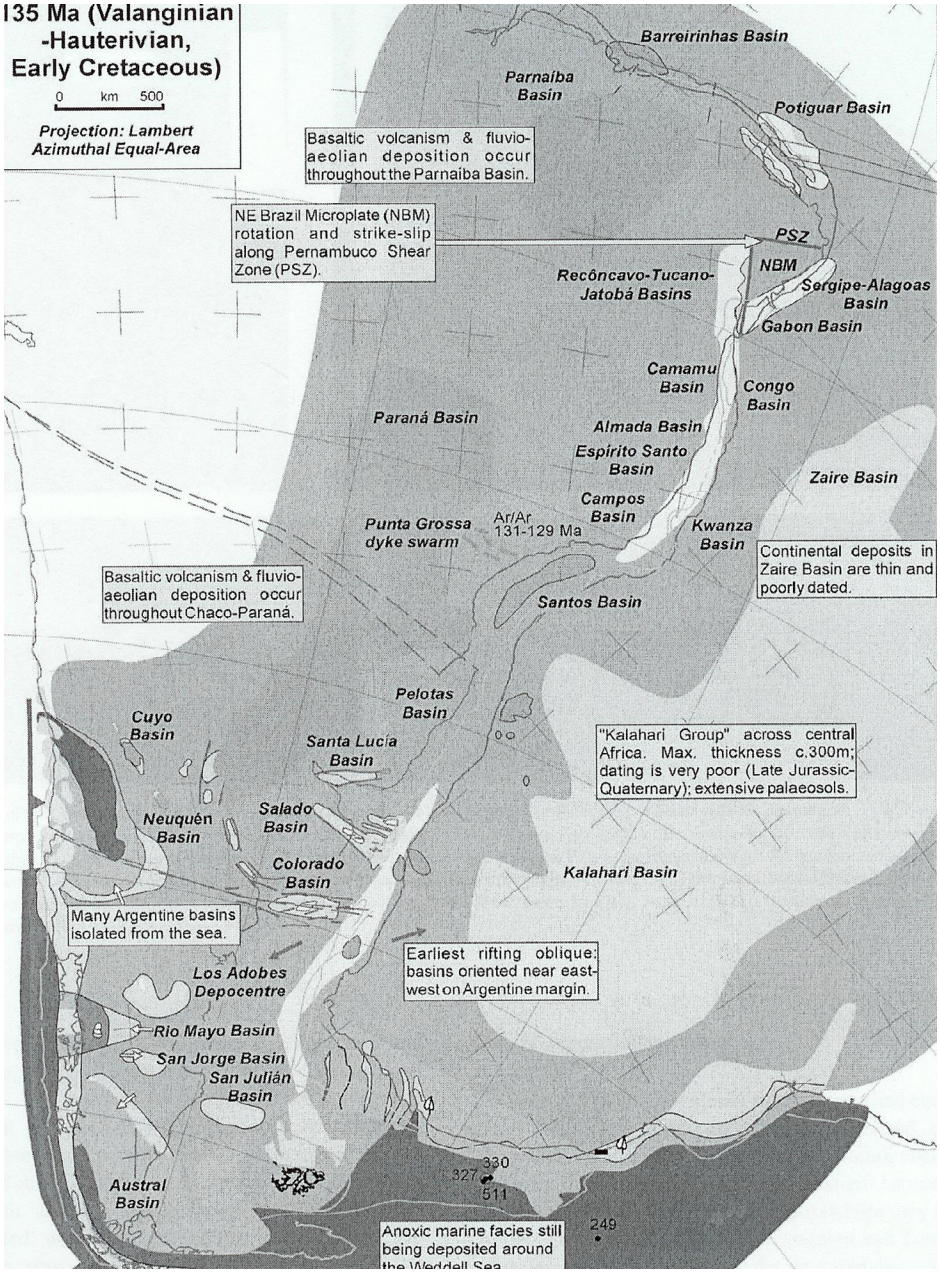

Figure 2.1. Reconstruction of the South Atlantic region at 135 Ma (Macdonald D. et al. 2002)

Pre-rift

Meyers et al. (1996) (and references therein) suggested a scenario of opening of the South Atlantic for the Gabon Basin, which can be applied to the study area of this work because of the scale of structures involved in it. This scenario includes existence of lithospheric weaknesses along NW-SE-trending Transamazonian (Early Proterozoic) and Pan-Africa/Braziliano (uppermost Proterozoic) suture zones within Gondwana. Tectonism that created Proterozoic sutures was followed by lithospheric stretching beneath Proterozoic collision zones and associated NE-SW-oriented extension starting at Late Jurassic, with formation of the Afro-Brazilian depression. In the Neocomian, increased rates of extension caused rift-block subsidence in the crust above the stretched lithosphere. Rifting between the Archaean Sao Francisco and Congo cratons was favored by lithospheric weakness and was directed by the youngest Transamazonian and Pan-African collision sutures (Meyers et al., 1996).

Meyers et al. (1996) pointed out that several elements including composite cratons, younger Gondwanide structural trends, thermal rejuvenation events, sediment cycles and intrusive zones for Brazil and West Africa are generally correlative, although apparent differences in opposing Precambrian terrains exist. Among possible reasons for the differences they preferred rejuvenation of terrains that caused subsequent thermal overprinting and isotopic adjustments, while Contrucci et al. (2004) and M. Mouline et al (2005) (and references therein) add to possible reasons intraplate deformation in both African and South American plates.

Rifting

Continental rifting started at approximately 150 Ma at the southernmost tip of the Southern Atlantic and propagated northwards. The area immediately south of the Walvis Ridge was reached at 126.5 Ma and the Benue Trough at 118.7 Ma. (Fig. 2.1 and 2.2) (Macdonald et al, 2002). Figure 2.1 shows that oblique extension has started in the southernmost South Atlantic, while Figure 2.2 depicts that most of the margins are in the thermal sag phase (after breakup) and have been transgressed. The Walvis Ridge has been overtopped and the northern part of the South Atlantic is now dominated by carbonate platforms. Rifting continued into the Barremian with creation of hinge zones and syn-rift basins.

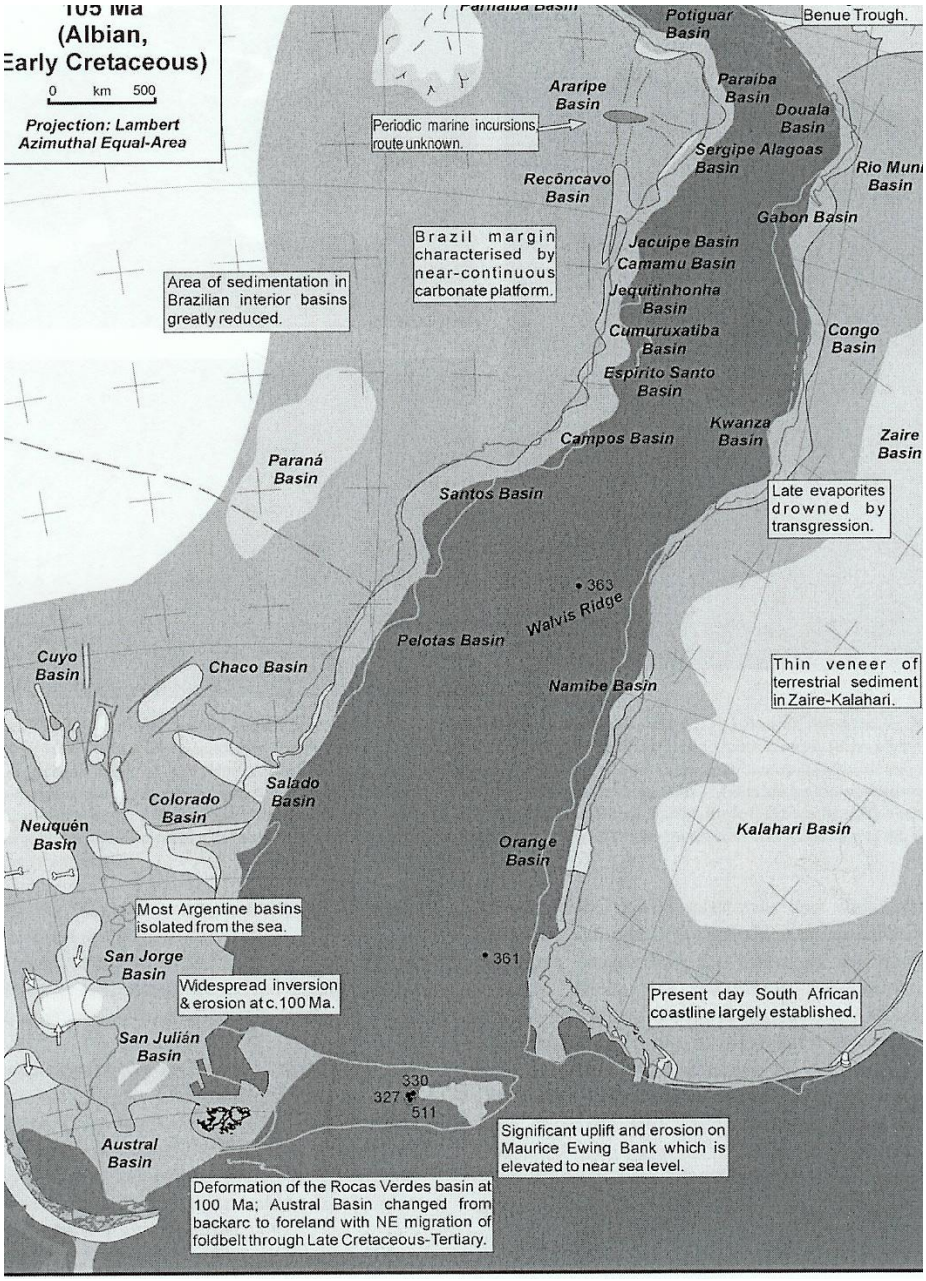

Figure 2.2. Reconstruction of the South Atlantic region at 105 Ma (Macdonald D. et al. 2002)

Karner & Driscoll (1999) recognized three rift phases associated with the breakup of Gondwana, with each phase being recorded by an onlap surface followed by an overall regressive package representing the subsequent infilling of the basin. Moulin et al. (2005) accepted that rifting started at the beginning of Neocomian (144.2 Ma) and tectonic activity ceased on the platform at the Intra-Barremian, whereas it continued in the basin. Howerver, they argue against the proposal of Karner & Driscoll (1999) of rift propagation along and across the region as a function of space and time. They point out that even if the tectonic

activity on the platform and in the basin stopped at different times, there is no evidence that they could not have both started during the same period (Early Neocomian).

Within the study area, Contrucci et al. (2004) differentiate two phases of continental rifting, which extended from the Neocomian to the Early Aptian. The first phase lasted from Neocomian to mid-Barremian and was characterized by extensional block faulting, and the second phase, from the mid-Barremian to the Early Aptian, was characterized by lesser tectonic activity.

Gjelberg & Valle (2003) proposed the subdivision of rifting into three phases that resembles the subdivision of Karner & Driscoll (1999), including:

1. The first phase - Berriasian to Hauterivian, was characterized by domal uplift and erosion associated with flexural downwarping, and the development of the Eastern Hinge margin and initial lakes.
2. The second phase – Hauterivian to mid-Barremian, was characterized as the rift climax. This was the phase of final breakup of Gondwana and establishment of Atlantic Hinge, located approximately 90 km to the west of the Eastern Hinge. Extensive hard salted water lakes developed in grabens and half grabens. Emplacement of oceanic crust took place along the breakup line.
3. The third phase – Late Barremian, is characterized by reactivation of both the Eastern Hinge and the Atlantic Hinge accompanied with the development of a major syn-rift unconformity (final breakup unconformity).

Spathopoulos (1996) recognized the syn-rift period, from Early Neocomian to Aptian, when normal faulting produced rift grabens and basement – tilted fault blocks. According to Meyers et al. (1996), intracontinental rift basins in the South Gabon Basin (to the north from the study area) began to develop during Neocomian along rift branches contemporaneous on the West-African and Brazilian sides. Rifting extended to early Aptian, as isolated rift basins in the South Atlantic began to be linked together across accommodation zones or transfer fault zones to form continuous rift basins. It is also argued that the entire South Atlantic rift system became joined in late Barremian to early Aptian (e.g. Spathopoulos, 1996).

Breakup of Gondwana and Atlantic opening

There is absence of any well-identified magnetic anomaly between Chrons C34 and M0 ("magnetic quiet zone") for the region to which the study area belongs, that makes it impossible to date the early stages of seafloor spreading from magnetic data. Breakup timing is based mostly on the age of breakup unconformity. Karner et al. (1999) assigned the final breakup to the second rifting phase, (rift climax) during Hauterivian to mid Barremian time, while Gjelberg & Valle (2003) placed the final breakup unconformity in early-mid-Aptian time. Furthermore, Moulin et al. (2005) dated the start of the South Atlantic Ocean opening at 140 Ma (Berriasian, Early Cretaceous) during the western Gondwana breakup.

Initiation of seafloor spreading to the north of the study area, in Gabon Basin, occurred sometime between the end of the Barremian and the early Aptian (Meyers et al., 1996). During the early Aptian, continental rifting ceased and subsidence tilted the margin westward, causing formation of a breakup unconformity. It is argued that final continental rupture (breakup) probably occurred at 112 Ma, coeval with the breakup unconformity onshore and below the shelf (Meyers et al., 1996).

Similarly, several studies have pointed out the asymmetric, "zip" pattern of continental rupture/plate separation (Marton et al., 2000; Contrucci et al., 2004). Wide zones on African side conjugate with narrow zones on Brazilian side and vice verce. For example, a wide zone (>200 km) of attenuated crust underlying the Gabon margin is conjugated to a narrow zone offshore Brazil (Meyers et al., 1996). According to Meyers et al. (1996) breakup was associated with anticlockwise rotation of the southern African plate with respect to the South American plate with a pole position ranging between 18°-27° N latitude and 18°W-2°E longitude. Rotation caused progressive, south-to-north opening of the South Atlantic along a NE-SW-oriented extensional stress field. Also, Rabinowitz & Labrecque (1979) indicated clockwise rotation of the South American Plate relative to the fixed African Plate.

Post-rift (drift)

The end of the rift period and transition to passive margin settings were marked by formation of the breakup unconformity and succeeding deposition of coarse clastic sequences. The post-

rift evolution of the African margin was mostly controlled by thermal subsidence that resulted in a general deepening of the basins and intensive salt tectonics.

Sea floor spreading continued to the east with the development of early post-rift sag basins and possibly the first marine incursion. During mid and late Aptian, extensive marine incursion into the restricted marine basins resulted in deposition of thick salt packages. Extensive salt packages separate the mainly continental sediments underneath from the marine sediments above thus forming an important regional marker and indicating fundamental change from continental settings to marine settings.

Several studies in the area have introduced concepts of salt tectonics or "raft tectonics". In particular Spathopoulos (1996) (and references therein) described "raft tectonics" as downslope movement of rigid blocks of sediments due to gravity-driven sliding on a décollement layer (usually evaporites or shales). It is a thin-skinned tectonic process whereby the footwalls and hanging walls of fault blocks become completely separated. The fault blocks are then called "rafts". The downslope movement produces listric faults and grabens. These grabens are filled with syn-deformational strata and can be extensive in dimensions, e.g. the Quenguela Graben in the Kwanza Basin is 20 km wide and 90 km long. The thickness of the décollement evaporitic layer is progressively reduced due to downslope salt flow. When most of the salt is removed under the fault blocks, their downslope movement will cease and they will be welded (or grounded) on the pre-salt layers. Figure 2.3 (Valle et al. 2001) depicts the development of rafting from the thin-skinned rafting stage where small blocks are involved to the thick-skinned rafting stage, with large-scale blocks.

Gjelberg & Valle (2003) defined the time from late Aptian to Present as the "drift period" and subdivided into Early-, Mid- and Late drift phases.

- *Early drift* was dominated by major thermal subsidence and sag basin development. Contractional tectonics are related to ridge push. There is evidence for volcanic activity in the southern part of the study area.
- During *Mid-drift* phase (from Late Cretaceous) subsidence in the west continued and was accompanied by uplift in the east. That resulted in a subtle tilting of the margin slope that initiated the thin-skinned rafting and development of a serious of small salt

detached listric faults and fault blocks rotation. In the areas with a thick salt layer, salt diapirs and pillows were developed.

- *Late drift* started at the transition between Eocene and Early Oligocene. The slope gradient of the margin increased due to uplift in the east related to the African superswell and continuous thermal subsidence in the west. Slope failure, slumps and debris flows occurred as a result of increased gradient. The increased dip of the margin slope and relatively thick overburden caused extensive Miocene thick-skinned rafting with creation of large-scaled raft blocks and raft grabens formation. Large-scale rafting led to the creation of local depressions on sea floor with coarse-grain infill (Valle et al., 2003). Steepening of the slope was combined with differential loading in areas with high sediment input.

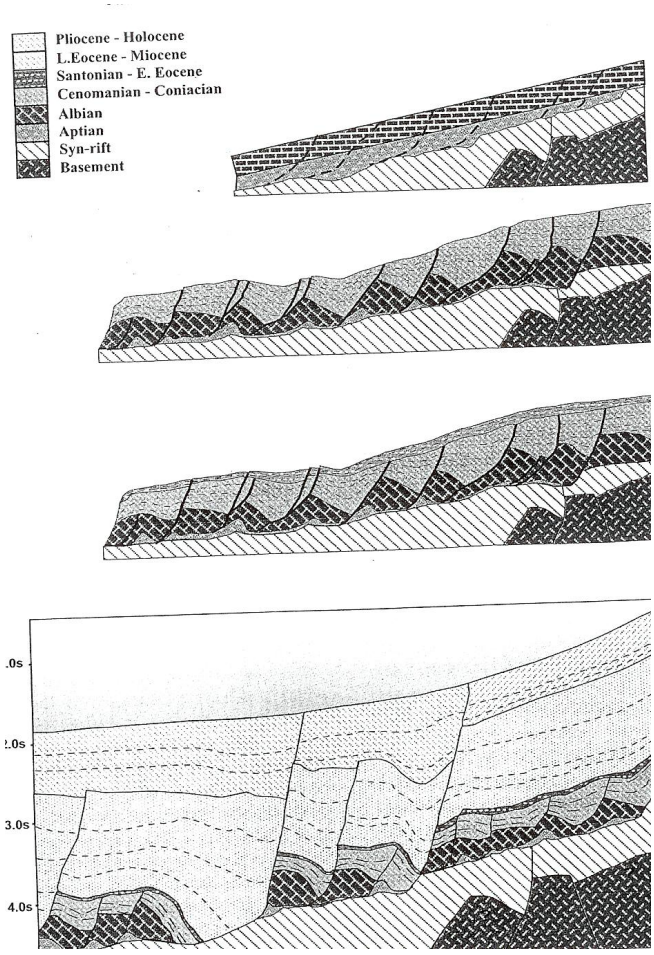

Figure 2.3. Development of rafts – thin-skinned rafting (upper) and thick-skinned rafting (lower) (Valle et al. 2001)

Several studies have pointed out the dramatic increase of sediment influx and consequent increased subsidence due to sediment load that started from Miocene. (Karner & Driscoll, 1999; Marton et al., 2000; Valle et al., 2001, 2003; Gjelberg & Valle, 2003). At that time, formation of the Congo Fan as an extensive depocentre took place. At the margins of the fan extensive salt walls developed with orientation parallel or tangential to the prograding front.
Several episodes of rotation of the margin took place during the Tertiary resulting in formation of unconformities in the uplifted parts to the east and creation of considerable accommodation space in the deep-water parts to the west where erosional material was successively redeposited. A significant basinwide unconformity developed in Early Tertiary. Considerable uplift during Miocene and later subjected the onshore areas of Kwanza Basin to severe erosion when up to 2000 m of sediments were eroded. Intensive uplift and relative sea-level fall from the end of the Miocene caused exposure of the shelf and sediment by-pass into the deeper areas (Gjelberg &Valle, 2003). Large-scale raft grabens development continued resulting in creation of local depressions on sea floor.

Volcanism

Gjelberg & Valle (2003) refer to undated volcanics as a part of the strata underlying the syn-rift group. Volcanism during the rift stages was associated with thick lava successions that are preserved in most of the fault bounded basins, and have been penetrated by several wells. Volcanic activity followed emplacement of oceanic crust during the second rift stage. Basalts and lava flows of the third rift (Late Barremian) stage probably formed highs within the lakes systems. On the simplified tectonic map of the study area (Fig. 2.4) (Marton et al., 2000) a volcanic line-chain is shown in the southern part. Furthermore, Meyers et al. (1996), describe outer highs in the Gabon Basin and, explain their origin by possible inferred volcanic intrusion. They compare the region with Red Sea, where it is believed that dike injections into thinned continental basement took place during its extension until continental crust became thin enough in places to give way to seafloor spreading. Detailed studies in the area of the Lower Congo Basin (Contrucci et al., 2004; Moulin et al., 2005) showed that the seismic structure of Angolan margin is very different from the one found at a typical rifted volcanic margins. MCS data indicated absence of seaward dipping reflections (SDR) similar to the Namibian margin, southward from the study area. Based on refraction data, it was concluded that volcanism is likely to have taken place but it is not a major process for the formation of

the margin. The thermal conditions that finally resulted in crustal thinning did not produce massive volcanic sequences.

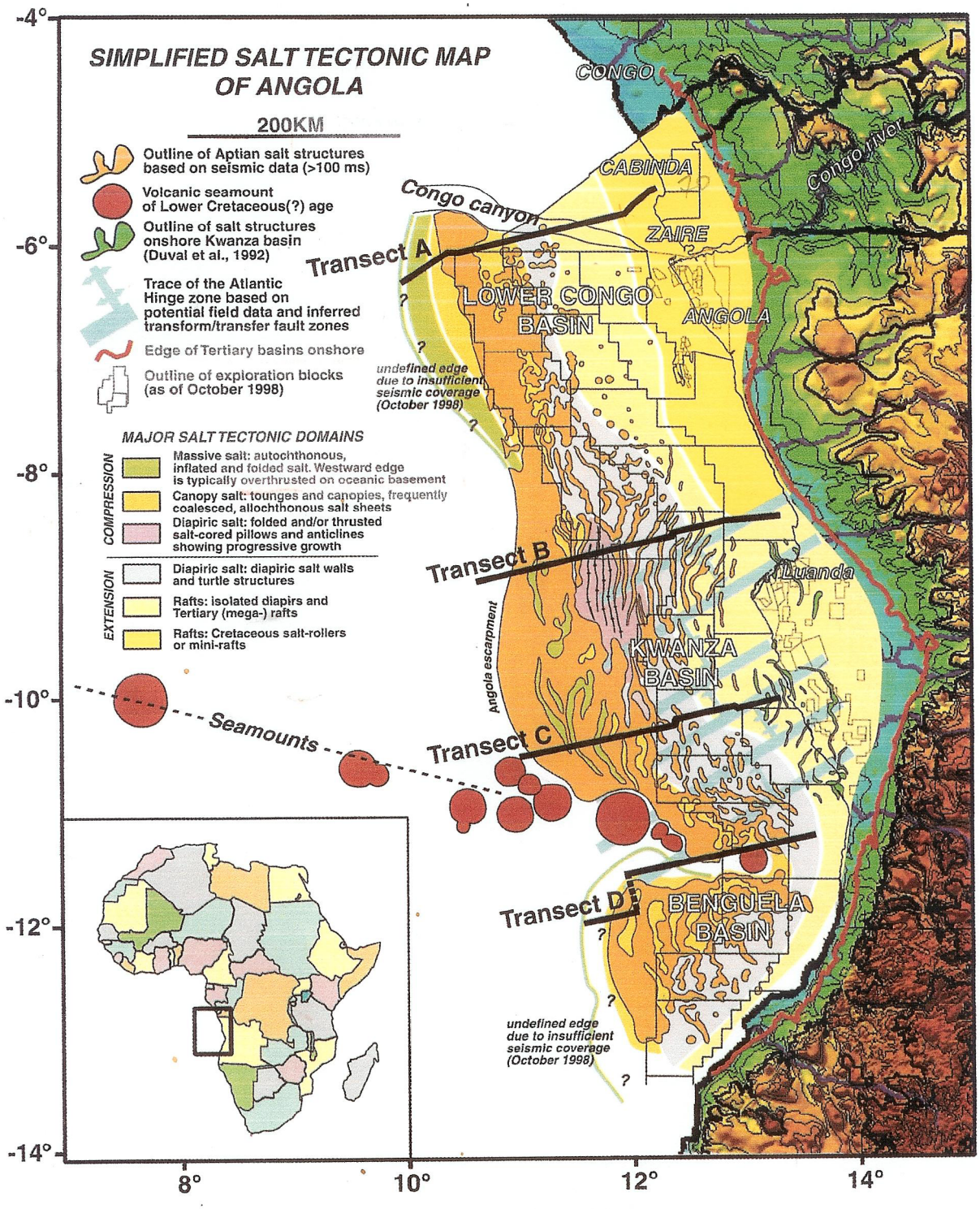

Figure 2.4. Simplified tectonic map with location of the four published MCS transects used in this study (Marton et al. 2000).

2.2 Angola margin

Geological provinces and structural features

Salt related provinces

With respect to salt related deformation the study area can be divided into four provinces (Gjelberg & Valle, 2003):

1. an area of mainly small scale thin-skinned raft blocks and salt detached listric faults,
2. mainly detached large scale raft blocks,
3. salt diapirs and salt walls,
4. thick diapirs and massive salt walls.

Duval et al. (1992) divided the Angolan margin into a region with dominating extensional regime in the east and a region with dominating compressional regime in the west. Finally, Spathopoulos (1996) provides the following description of the salt-related provinces:

Extensional provinces. The *unrafted province* exists onshore and the eastern part of the offshore Angola. Here Albian-Cenomanian prerafts (blocks bounded by listric faults but not separated) covered by Upper Cretaceous-Eocene strata. Listric faults do not continue upwards through Upper Cretaceous. The *raft province* lies to the west of the unrafted region. Large, basinward dipping listric faults sole out on the salt layer, but are not directly connected with structural features within the pre-salt section. This province is characterized by large-scale rafts and grabens, later filled with Tertiary sediments, usually turbidites. The salt layer is very thin or absent.

Contractional provinces. The *salt diapir province* is located to the west of the raft province, with water depths more than 500 m. The province is characterized by several salt diapirs, each about 5 km in diameter, which have pierced the folded rafts. Diapirs are connected to form salt walls. The salt layer reaches thickness of 300 m. The *salt swell province* is the westward continuation of the diapir province and lies in water depths of more than 1000 m. It is characterized by a very thick evaporate layer (1000-2000 ms) with salt swells and diapirs on top. The post-salt sedimentary layer is strongly faulted and folded. The abrupt change in thickness of the salt layer is attributed to the basinward expulsion of the salt under the prograding Tertiary sedimentary wedges. The *tabular salt province* lies in water depths of

more than 1500 m. It is characterised by a thick (1500-200 ms) evaporitic layer. The top of the salt layer is almost flat. The sedimentary successions overlain salt are almost undisturbed.

Spathopoulos (1996) indicated that the areal distribution of the above provinces changes significantly along the strike of the margin. Abrupt variations in the width of the unrafted and raft provinces as well as in the style of raft tectonics occur over small distances and divide the margin into distinct tectonic segments (Fig. 2.5).

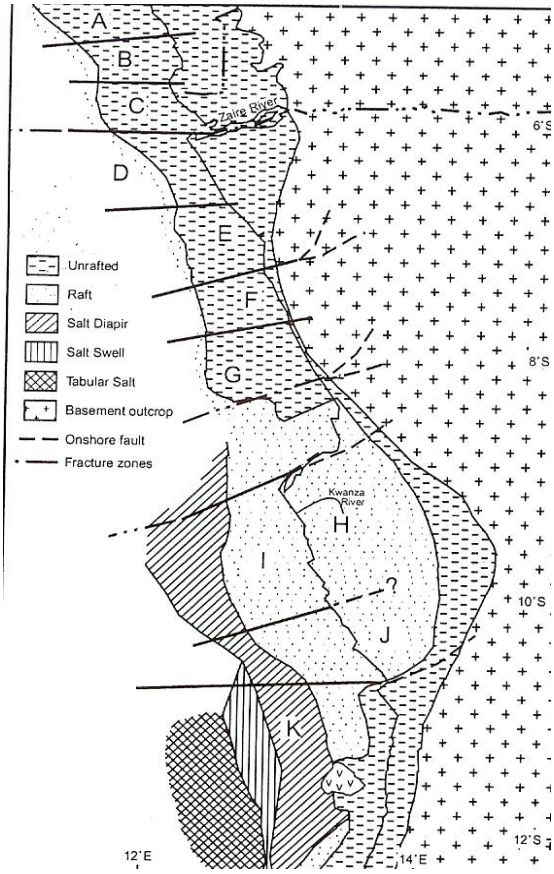

Figure 2.5. Areal distribution of the different salt provinces (Spathopoulos, 1996).

Deformation of Aptian salt across the margin was controlled by differential subsidence above pre-existing rifted structures. Salt was originally deposited as a relatively continuous layer on a shallow basin margin with gentle slope. The Aptian salt basin gradually deepened to the south-west. Intensive basinward thickening of the salt took place after deposition due to down slope squeezing of salt by prograding sediment wedge. Meyers et al. (1996) as well as other authors point to the lack of deformation in sediments above salt near the seaward edge. It is suggested that salt was originally autochthonous over the outer highs, implying salt deposition contemporaneous with the final continental rupture and emplacement of proto-oceanic crust.

Meyers et al. (1996) proposed overall "staircase" geometry of the salt base for the Gabon Basin due to continued tilting and differential subsidence between rifted crustal blocks during/after salt deposition.

Crustal provinces

Investigation using vertical reflection and wide-angle reflection-refraction techniques in the Lower Congo Basin (Contrucci et al., 2004; Moulin et al., 2005), resulted in the subdividsion of the area into four crustal zones/provinces (Fig. 2.6):

- *Zone I* corresponds to a continental platform domain and consists of minor extended, 30- to 40 km thick continental crust.
- *Zone II* is the continental slope domain; about 50 km wide. It can be subdivided into three subzones, characterized by different basement slope angles: 11°, 22° and 11°, respectively. Deepening of the basement top occurs within a distance of 50 km, from 3 km to 10 km in depth, overall to 7 km. The few observed tilted blocks have a lateral dimension about 10 km and maximum offset 2-4 km. Thickness of pre-salt layer ranges from about 500 m in the east to 5 km in the west.
- *Zone III* is a transitional domain between foot of the continental slope and what can be unequivocally defined as the oceanic crust. Its length is about 160 km. Contrucci et al. (2004) and Moulin et al. (2005) pointed out that within subsalt sedimentary layer no extensional faulting took place, which indicates absence of any significant extensional tectonic motions. The thickness of pre-salt layer is 2-4 km, and the thickness of the crust is 3-10 km. Within this zone strong reflectors were defined as an "anomalous velocity layer", which is visible from the east to middle of the zone and is not visible in the western part, where it cannot be imaged due to masking effect of salt. In this transitional domain, the crust can neither be recognized as oceanic, nor as continental.
- *Zone IV* is the ocean crust domain with thickness of about 7 km.

The thickness of the crust changes abruptly over a distance of less than 50 km, from a thickness of 30-40 km in zone II below the continental platform to less than 5 km at the slope foot. The maximum thickness, about 6 km, is located below the post-salt sediment depocentre. No imprint of significant extension is observed to explain this abrupt crustal thinning. Parallel reflectors within the subsalt layer indicate that deposition occurred while the

basin was subsiding vertically without any flexure. Contrucci et al. (2004) and Moulin et al. (2005) postulated that the Lower Congo Basin appears to have been mainly formed vertically; vertical motions prevail compared to horizontal motions. This excludes any stretching processes and points to either inherited very thin continental crust or more likely to lower crust thinning processes.

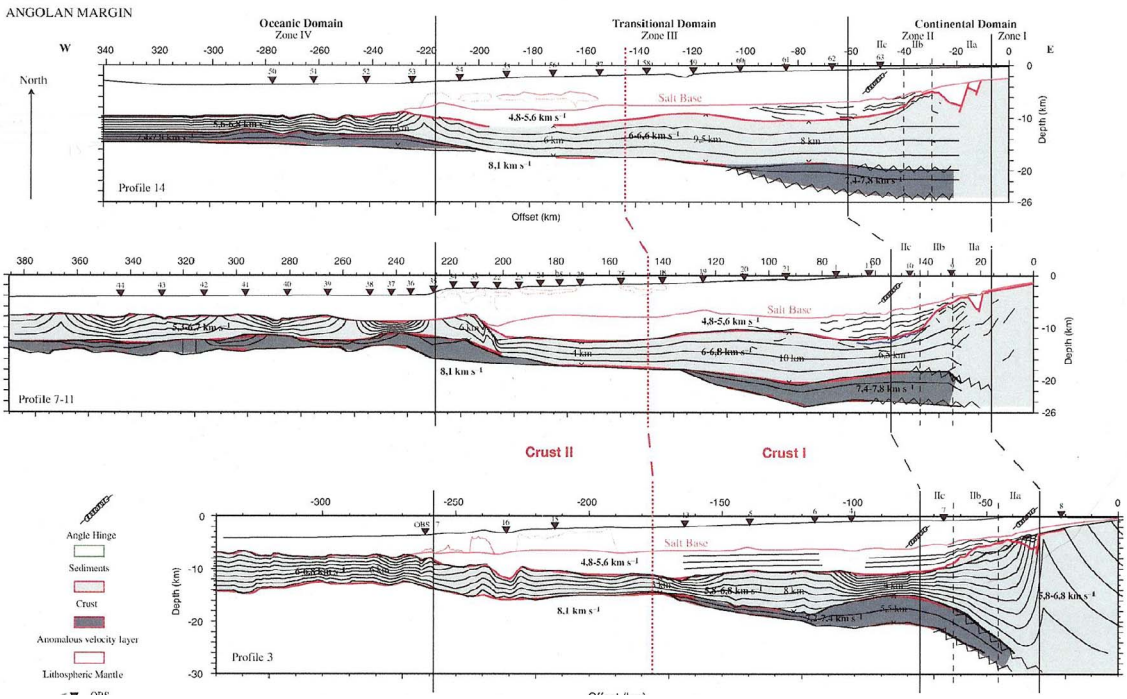

Figure 2.6. The different structural domains and Zones I-IV (Moulin et al. 2005).

The transitional crust is divided into two parts, Type I and Type II. Type I is made by the upper continental crust, while Type II could be an atypical oceanic crust, serpentized mantle, lower continental crust, or intruded continental crust. It was suggested a decoupling zone between an upper crust and ductile-deforming lower crust and lithospheric mantle (Meyers et al., 1996). Similarly, Contrucci et al. (2004) and Moulin et al. (2005) suggested that the existence of a detachment exhuming lower crust (Type II) from beneath the continental margin and exposing it in the deep basin is a good explanation of the structuration of the Angola margin.

Stratigraphy and geological evolution

Detailed litho-stratigraphic columns for the study area are presented in Figures 2.7 and 2.8 (Valle et al., 2003; Gjelberg & Valle, 2003).

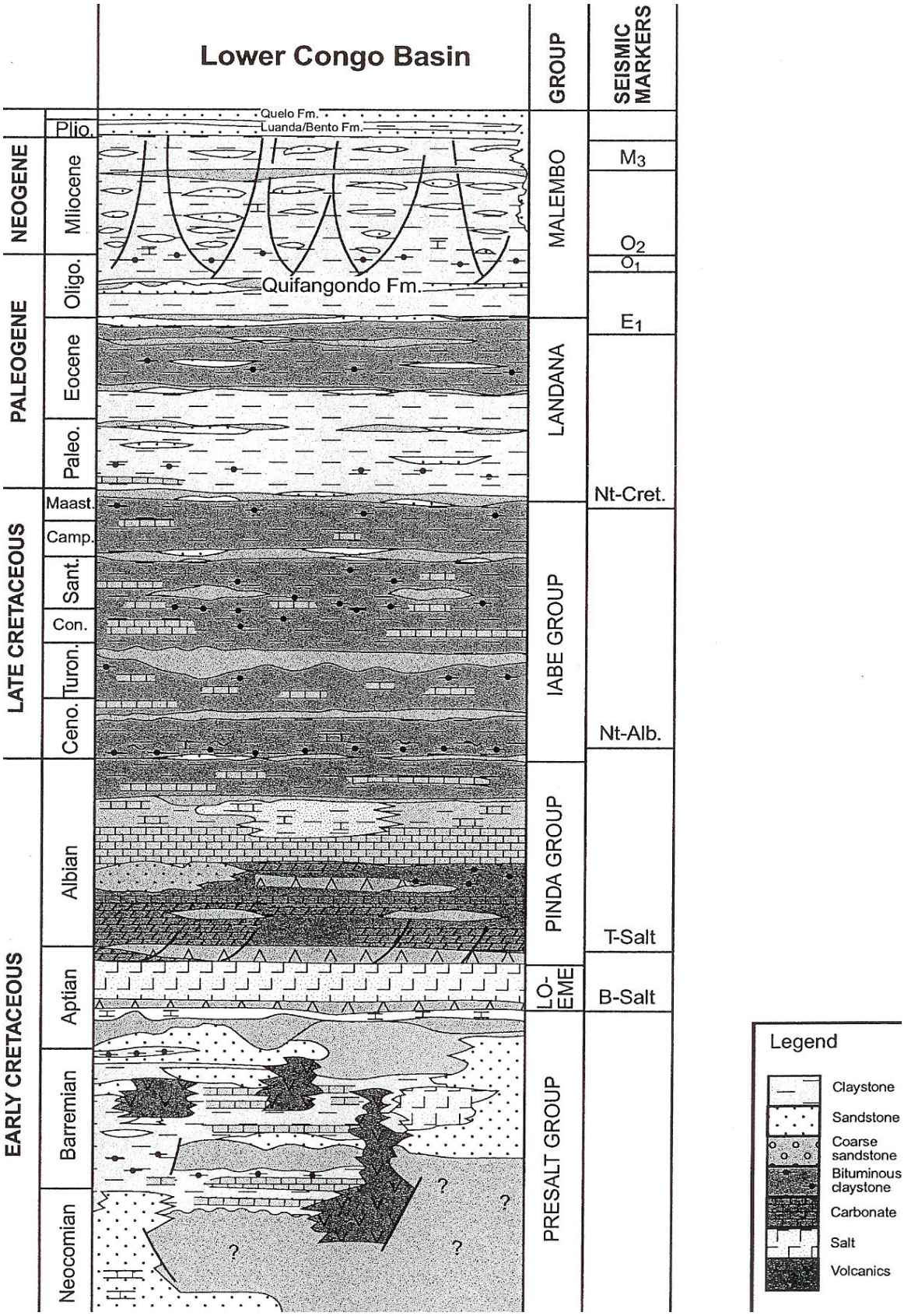

Figure 2.7. Litho-stratigraphic column for the Lower Congo Basin (Valle et al. 2003).

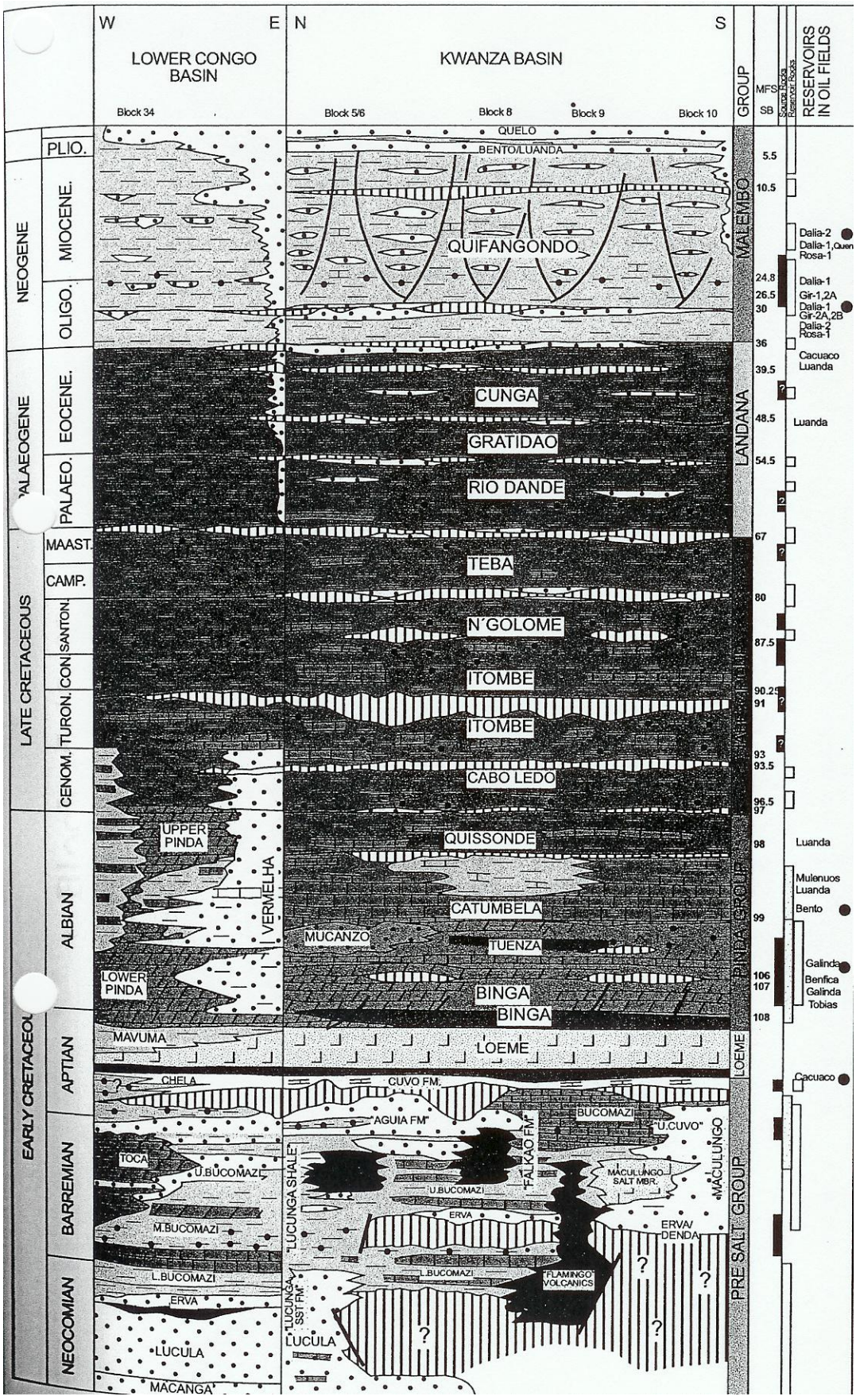

Figure 2.8. Litho-stratigraphic column for the Lower Congo Basin and the Kwanza Basin (Gjelberg & Valle, 2003).

The crystalline basement in the study area is considered of Precambrian age. It is mainly of metamorphic origin and consists, in general, of biotite and hornblende gneiss, and granites (Gjelberg & Valle, 2003).

Sediments of the syn-rift group are of Neocomian to Aptian age and were originated in continental settings. Active rifting initiated intensive faulting and creation of grabens and half-grabens. Lacustrine environments were established in syn-rift lakes with stagnant water conditions, which led to deposition of lacustrine shales and carbonates during the first rift stage and marls, limestones and organic-rich shales during the second and third rift stages. The latter represents the source rocks of this interval. Coarse-grained clastic alluvial fan deposits (sandstones and conglomerates) originated close to fault escarpments. The end of the rift period and conversion to passive margin settings are marked with successions of poorly sorted fluvial/deltaic sandstones interfingering with carbonates. These sequences are located below the main breakup unconformity and represent a gradual facies transition. Furthermore, sediment packages of conglomerates, sandstones of alluvial origin and shales of possibly shallow marine origin have been deposited above the breakup unconformity. The last mentioned sediment packages have an overall transgressive character reflecting marine incursion. They immediately underlie thick salt deposits (Marton et al. 2000).

During Aptian, restricted marine environments in the deepest parts of the basins with sabkha areas at the margins were established all over the region. Thick salt deposits were therefore accumulated. The primary salt thickness is largely argued. Generally, accumulations in the western parts of the salt basin were much thicker than in the eastern part. According to Gjelberg & Valle (2003), the primary salt thickness varied from >1000 m in the west to <50 m in the east.

The early drift was dominated by thermal subsidence. Shallow marine shelf environments were established, which led to the generation of a carbonate platform. The facies development has an overall transgressive character. These carbonates make the main reservoir rocks in Cabinda and Zair, northward from Angola offshore. Episodic anoxic bottom water conditions occurred during Early-mid Aptian when a good source rock interval was generated (Tuenza Fm, Kwanza Basin) (Gjelberg & Valle, 2003). In the beginning of mid drift stage the region represented a stable platform with slight westward tilting. Deposits originated during the mid

drift-stage consist dominantly of dark, grey to brownish claystones and siltstones, with intercalations of marls and carbonates, and represent shallow marine/shelf environment, later - deeper marine conditions. Short episodes with anoxic bottom water conditions were repeated during this time with depositions of organic-rich sequences, representing good candidates for source rocks. The maximum flooding surface is defined in the middle of mid rift stage and assigned to the boundary between the Itombe and the overlaying N'Golome formations (transition from Conician to Santonian) (Fig. 2.8).

Late Cretaceous uplift in the hinterland gave rise to a regional unconformity and slightly increased silicilastic input to the basin margins in the east. However, the period comprising the Cretaceous – Tertiary transition and the Palaeocene is generally characterised by a low sediment rate and condensed intervals. The depositional environment is interpreted as deep-marine shelf/slope with suboxic bottom conditions. In the Palaeocene (the beginning of late drift stage), mainly grey claystones and pale limestones were deposited. Intervals with relatively high organic content were generated (within wide-spread the Rio Dande Fm, both in Kwanza and Lower Congo Basins) (Gjelberg & Valle, 2003). These intervals may represent potential source rocks.

At the end of the Palaeocene, the depositional environment changed to an open marine shelf. A regional unconformity marks the transition between Eocene and Lower Oligocene indicating renewed uplift in the hinterland. During the Oligocene and the Miocene several episodes of regional hiatus occurred. Sedimentary sequences of Oligocene, Miocene and Pliocene to Recent are dominated by calcareous to non-calcareous claystones, siltstones, mudstones and sandstones. Extensive tilting of the basin floor in Oligocene and reactivated raft tectonics created highly sinuous deep-marine channels filled with turbidites and debris flow. Several series of thick sands of turbiditic- and shelf-origin occur at different levels within these sequences and represent important reservoirs. Valle et al. (2003) indicated that rotation of large-scale raft blocks produced local depressions on the sea floor thus implying local tectonic control on the distribution of turbiditic currents. Hence, the relation between sea floor relief actual for sedimentation and direction of sediment transport must be regarded as favourable for formation of potential reservoirs.

3. DATA AND METHODS / APPROACH

3.1 Data

The data used in this work were accumulated from different sources.

Published seismic profiles/transects

Four published seismic profiles (transects A, B, C and D; Figs. 3.1 and 3.2) from Marton et al., (2000) were used as a basis for constructing the two-dimensional earth model for 2D-gravity modelling. Transects are located between 6°S and 13°S, offshore Angola (Figures 2.4 and 3.1). The profiles are depth converted composite industry reflection seismic lines of different vintages, including acquisition of a high-quality regional 2D reflection seismic grid in the ultra-deep water area (water depths >1000 m). Interpretation of thesseismic data was constrained by basinward extrapolation of wells drilled on the continental shelf and by DSDP (Deep Sea Drilling Project) results. The length of the transects is generally 250-300 km and their depth is ~6-8 km. (Fig. 3.2). In Figure 3.3 the stratigraphic units along with average interval seismic velocities of the area are indicated, representing sedimentary sequences with generalised lithologies.

Publicly-available data sets

During this work the authoritative, publicly-available data sets for the world's oceans were utilised. They include:

1. High resolution ship-track measurements collected during research cruises (academic data: LDEO, Lamont-Doherty Earth Observatory, Columbia University, USA).
2. Gridded gravity data: 1x1 min gridded free-air satellite-radar-altimeter free-air gravity anomaly field (Sandwell & Smith, 1997 v.10.1).
3. Gridded bathymetry data:1x1 min elevation grid (GEBCO; Jakobsson et al., 2000). General Bathymetric Chart of the Oceans (GEBCO) operates under the auspices of the International Hydrographic Organisation (IHO) and the United Nations' (UNESCO)

Intergovernmental Oceanographic Commission (IOC). (http://www.ngdc.noaa.gov/mgg/gebco/gebco.html).

4. Total Sediment Thickness of the World's Oceans & Marginal Seas: a digital total sediment thickness database for the world's oceans and marginal seas is being compiled by the National Geophysical Data Center (NGDC). (http://www.ngdc.noaa.gov/mgg/sedthick/sedthick.html). A 5x5 min grid was utilized in this study.

3.2 Basemaps

The margin setting is depicted on the constructed basemaps including potential field grids, the coastal line, transects, profiles from relevant studies, and ship-borne tracks located within the study area. For that purposes the GMT software package (Generic Mapping Tools; Wessel & Smith, 1998) has been utilised. GMT is an academic, interactive software package that provides powerful tools for reduction, management, and visualization of geophysical data. It is possible to extract bathymetry, gravity anomaly data and magnetic anomaly data along cruises tracks and along lines from grids. GMT allows constructing maps from gridded data as well.

Figures 3.4-3.8 show the resulting maps of the study area, including the bathymetry (Fig. 3.4) and free-air gravity anomaly map (extracted from gridded data) (Fig. 3.3), Bouguer gravity anomaly map (calculated from gridded data) (Fig. 3.6), magnetic anomaly map (extracted from ship-borne data) (Fig. 3.7) and the sediment thickness map (extracted from gridded data) (Fig. 3.8). For the construction of the Bouguer-corrected gravity map, a density of 2.20 g/cm^3 was utilized as infill to the bathymetric relief. A density of 2.67 g/cm^3 was also tested and gave approximately the same result in a regional sense.

The ship-born tracks within the study area were investigated. Tracks or parts of tracks that are located along transects were chosen for further work and were plotted on the basemap. Additional profiles were superimposed on the basemap, such as profiles 1, 9, 3, 7+11, 12 and 14 from Contrucci et al. (2004). The resulting basemap of the study area with coastline, composite lines (in black), seismic transects (in red), profiles from Contrucci et al. (2004) (in blue), and tracks are

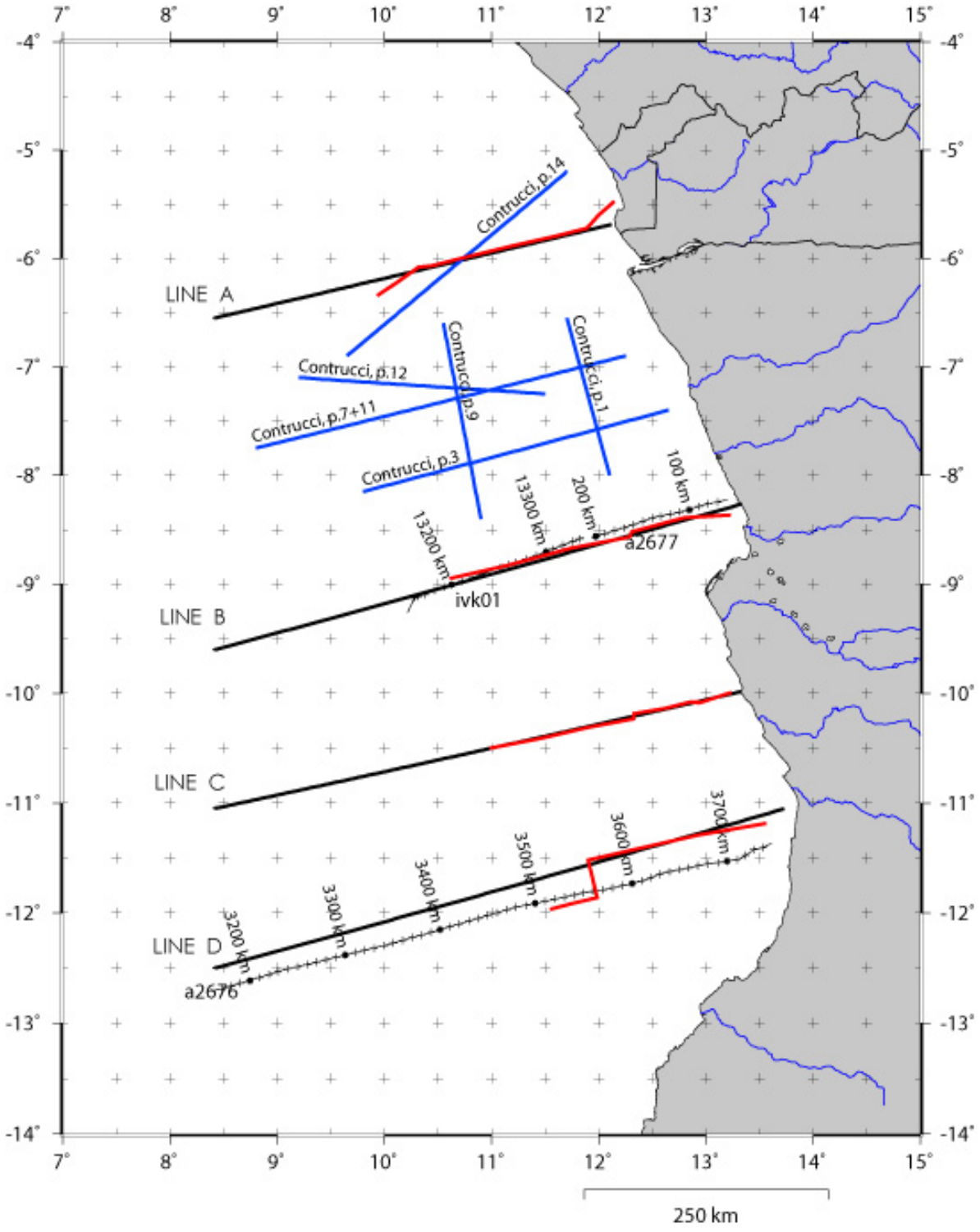

Figure 3.1. Basemap. Lines A, B, C, and D – composite lines used in this study; lines in red color – transects from Marton et al. (2005); lines in blue between 5°S and 9°S – profiles from Contrucci et al. (2004) and Moulin et al. (2005), lines indicated with ivk01, a2677 and a2676 – the parts of the ship-born tracks used in this study.

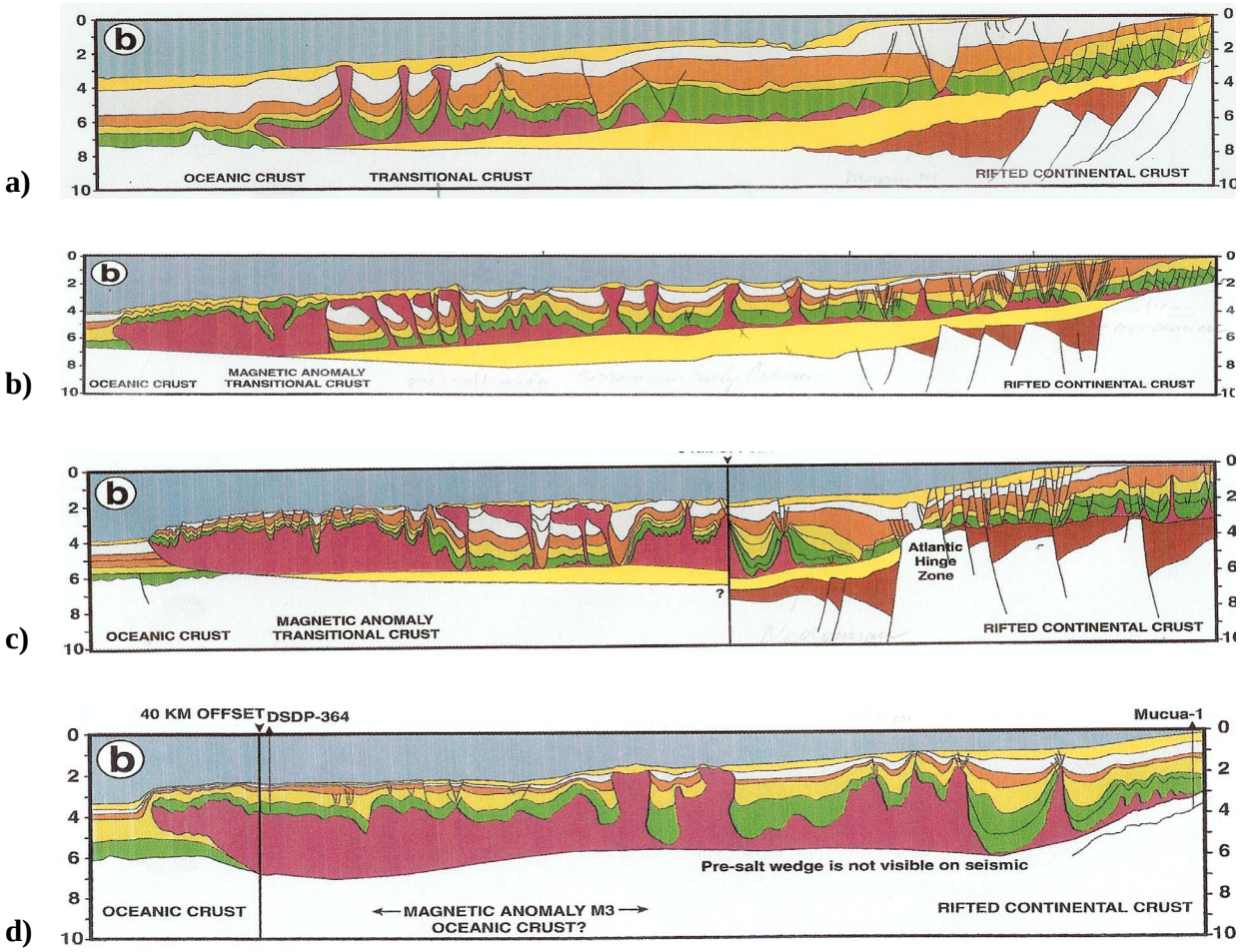

Figure 3.2. Four transects from Marton et al. (2000): a) transect A, b) transect B, c) transect C, d) transect D.

shown on Figure 3.1. The basemap was constructed in Mercator projection, within coordinates 4°S /14°S and 7°E /15°E.

3.3 Seismic interpretation and depth conversion

Based on the acquired experience with the geology of the study area, and in order to proceed further on with modelling, four depth converted seismic transects from Marton et al. (2000) were extended oceanward. These extended composite lines became the main seismic structure dataset of the study, including (Fig. 3.1):

- Line A - starting point 8.40° S / 6.55° E, azimuth 77, length 420km.
- Line B - starting point 8.40° S / 9.60° E, azimuth 75, length 560km.
- Line C - starting point 8.40° S / 10.6° E, azimuth 75, length 530km.
- Line D - starting point 8.40° S / 12.5° E, azimuth 75, length 600km.

Generally depth conversion follows seismic interpretation, where the seismic section in two-way traveltime (twt) is studied, interpreted and digitised. Subsequently, velocity-depth functions for the study area must be constructed using data from available well-logs, stacking velocities and regional lithologies. This means that the stratigraphy of the area has to be investigated, lithologies have to be defined, and seismic velocities for stratigraphical units have to be obtained. Interval velocities have to be defined at different intervals, e.g. every 10 km, along the interpreted seismic profile. With these values the velocity parameter file has to be constructed. The “in-house” software package SECTION (Planke, 1993) can be utilized for digitization, velocity parameter-file construction, and depth conversion.

For this study, depth converted transects were used. However, regional velocity information was gathered through published data. This is because seismic velocities are dependent on rock densities and these were, in turn, used in further gravity modelling of the four transects. Therefore, initial information about rock densities could be obtained by analyzing the seismic velocities of the stratigraphical units within the study area. Marton et al. (2000) provided interval seismic velocities within the study area (Fig.3.3). These velocity values were converted to densities by means of an empirical relationship between seismic velocities and densities of the rocks (Fig. 3.9). The stratigraphic units differentiated by Marton et al. (2000) have been assigned values according to their interval velocities. Table 3.1 shows the stratigraphic units of this work and their average values for density. Densities accepted for this work lie within range for rock densities from Dobrin and Savit (1988) (Table 3.2). The average densities used in this work will be explained and discussed later on.

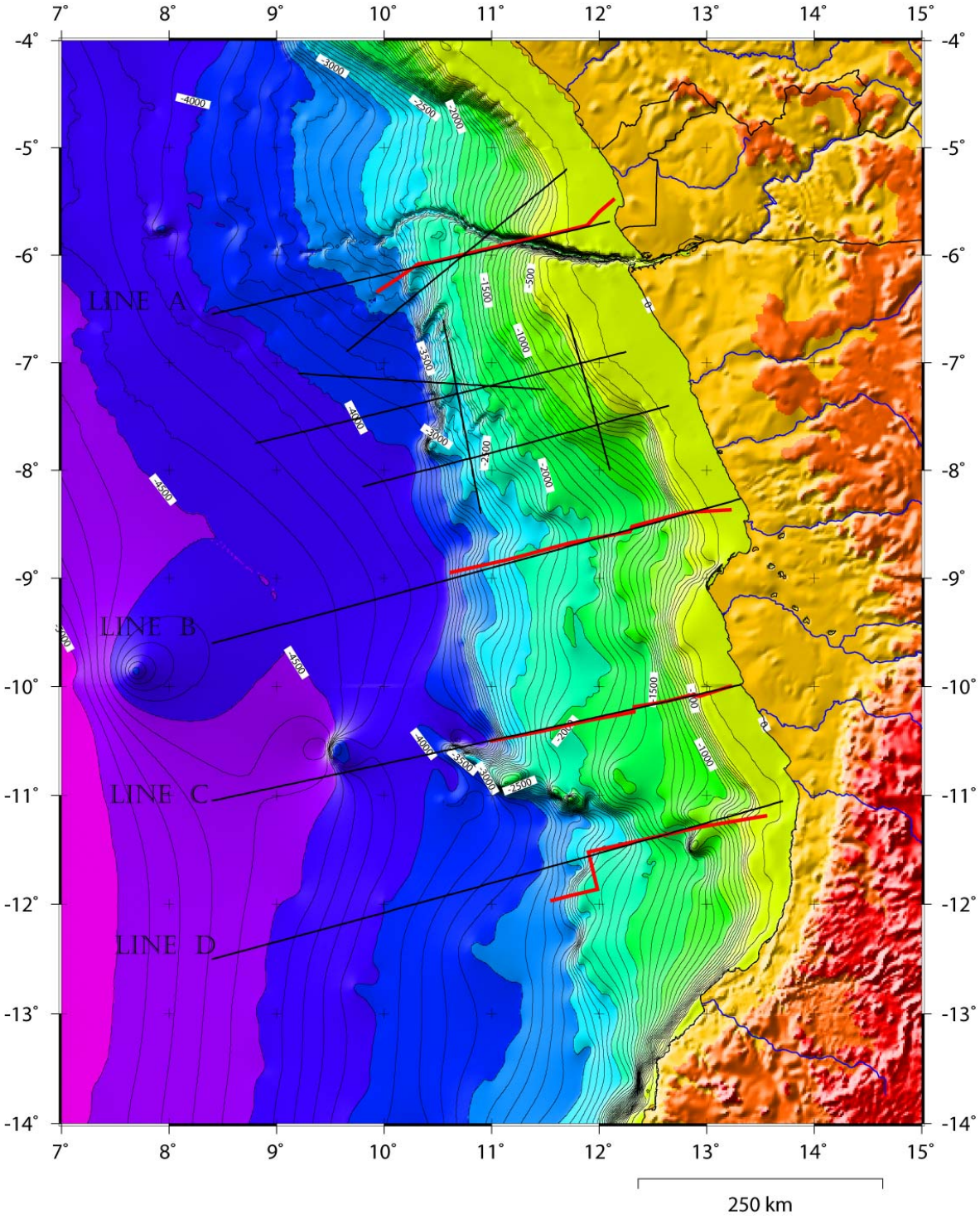

Figure 3.4. 1x1 minute elevation grid (GEBCO, General Bathymetric Chart of the Oceans; Jakobsson et al., 2000). Lines A, B, C, and D – composite lines used in this study; lines in red color – transects from Marton et al., (2005); lines in black between 5°S and 9°S – profiles from Contrucci et al., (2004) and Moulin et al., (2005).

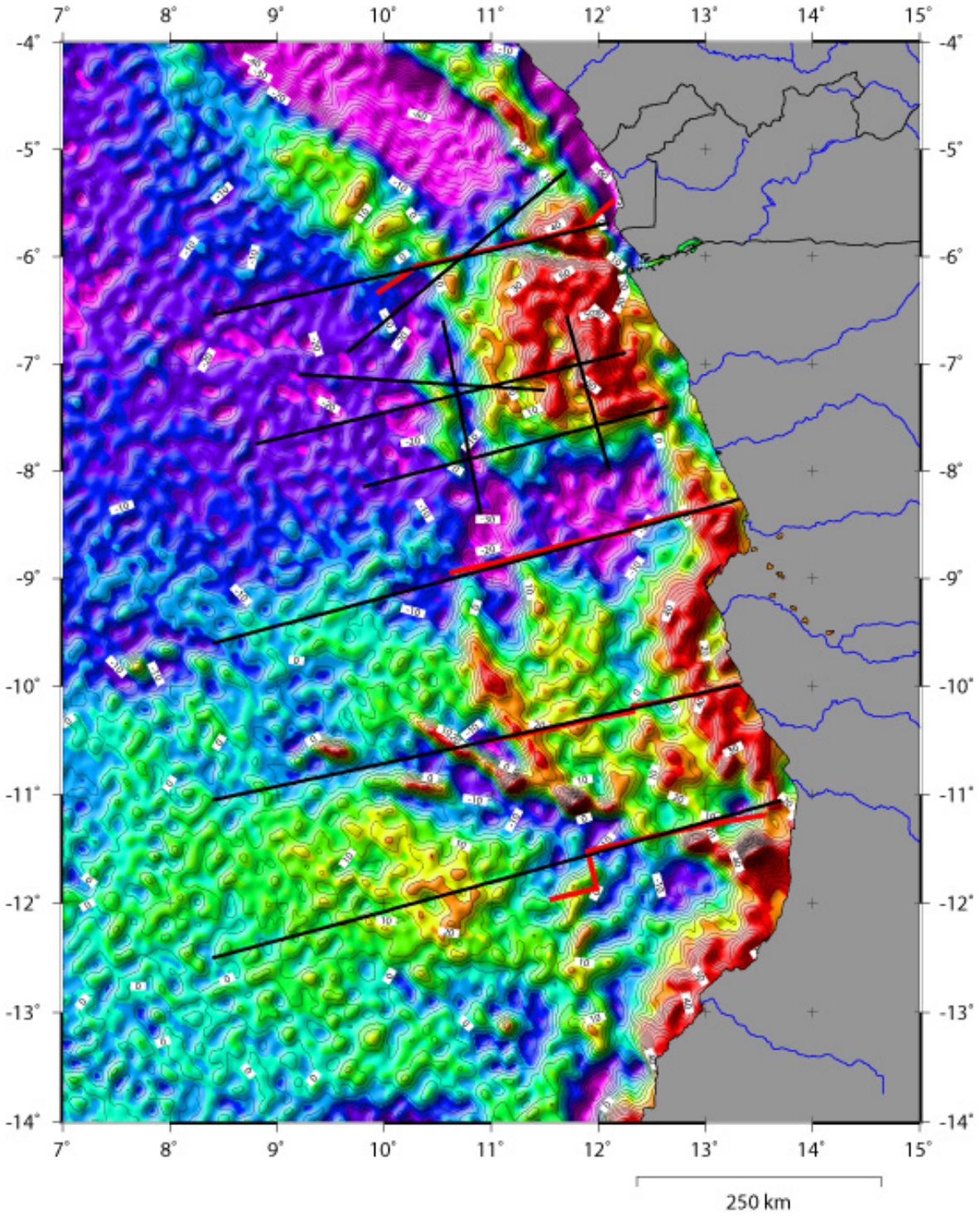

Figure 3.5. 1x1 min gridded free-air satellite-radar-altimeter free-air gravity anomaly field. (Sandwell & Smith, 1997 v.10.1). Lines A, B, C, and D – composite lines used in this study; lines in red color – transects from Marton et al., (2005); lines in black between 5°S and 9°S – profiles from Contrucci et al., (2004) and Moulin et al., (2005).

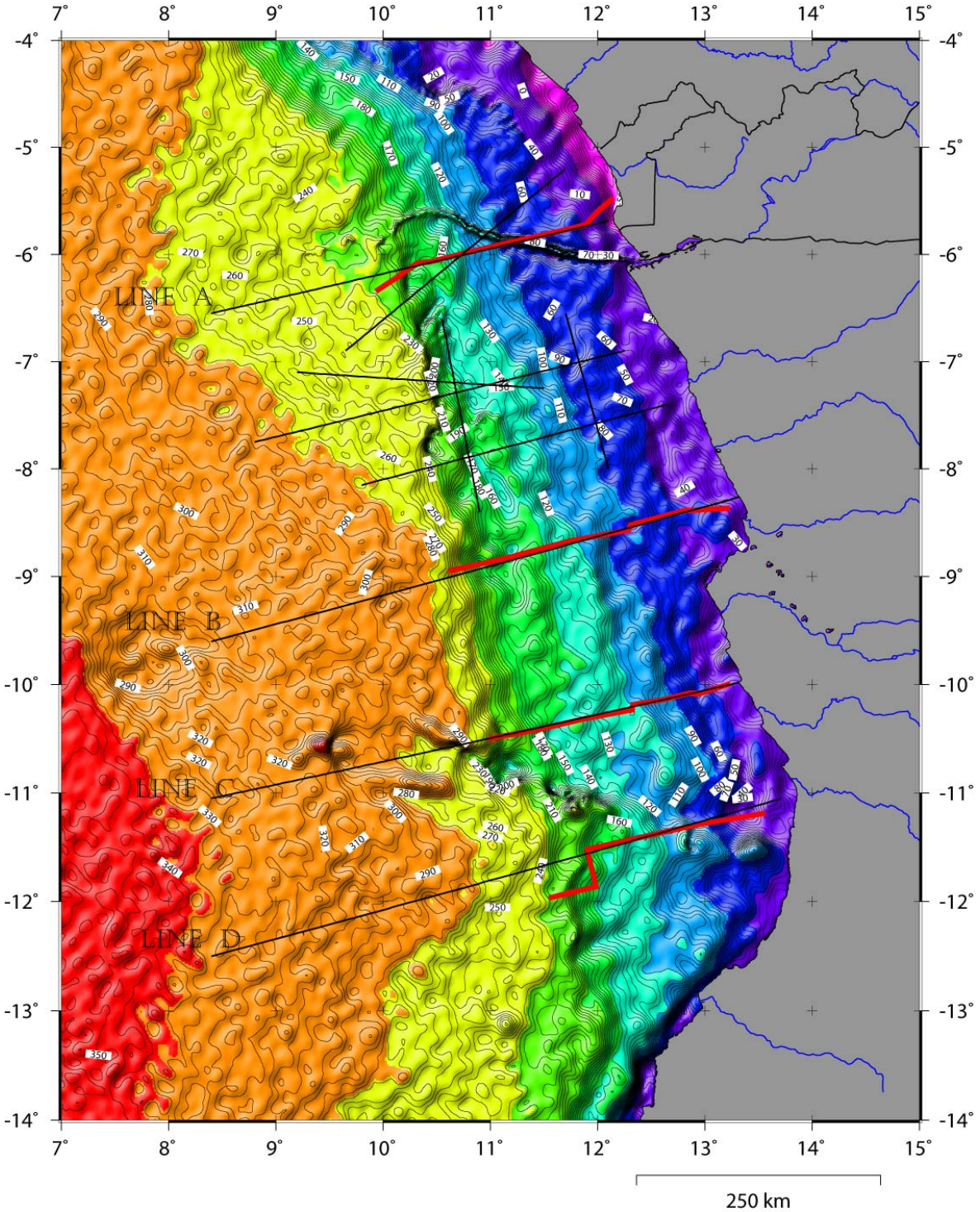

Figure 3.6. Bouguer gravity anomaly map. Lines A, B, C, and D – composite lines used in this study; lines in red color – transects from Marton et al., (2005); lines in black between 5°S and 9°S – profiles from Contrucci et al., (2004) and Moulin et al., (2005).

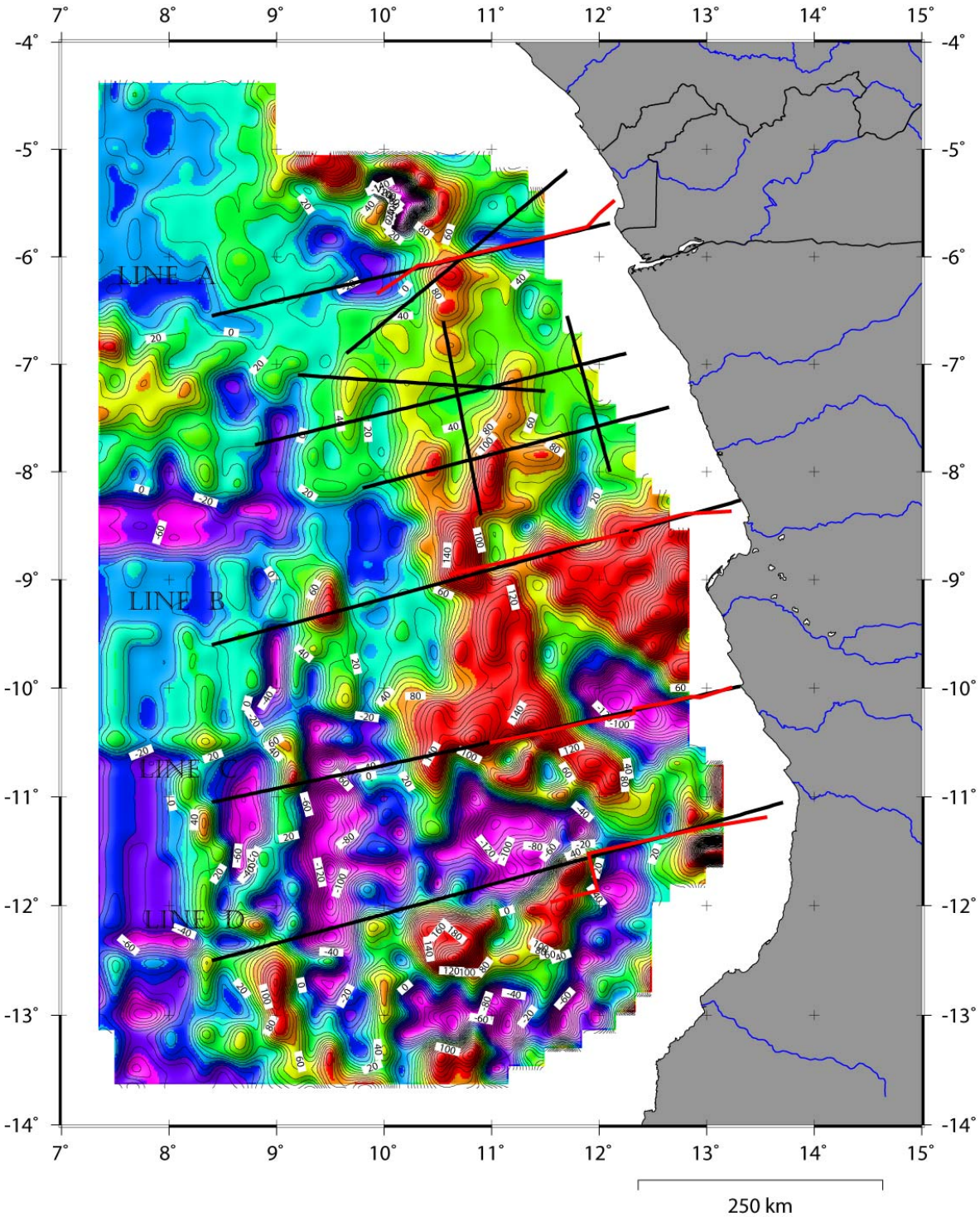

Figure 3.7. Magnetics. Lines A, B, C, and D – composite lines used in this study; lines in red color – transects from Marton et al., (2005); lines in black between 5°S and 9°S – profiles from Contrucci et al., (2004) and Moulin et al., (2005).

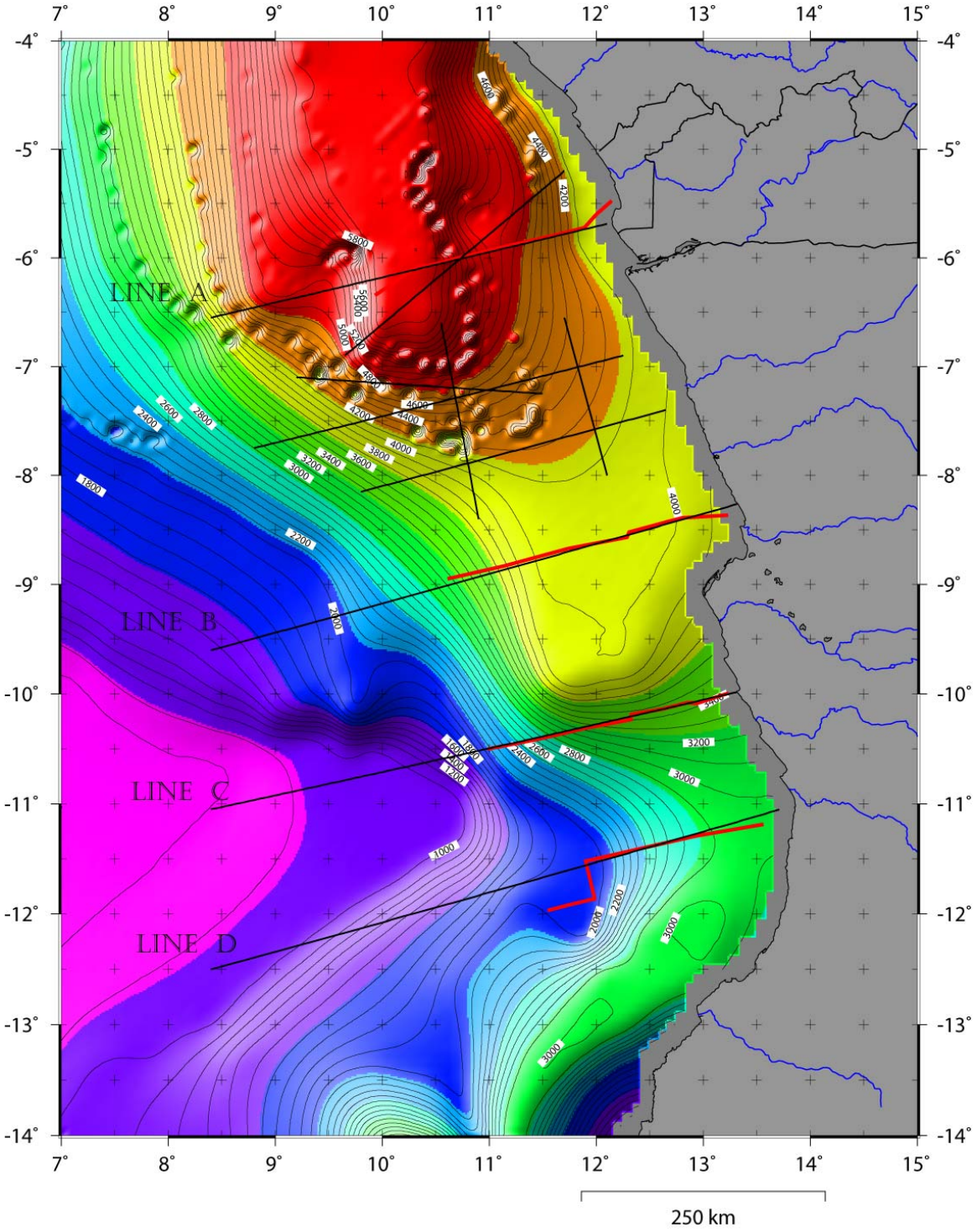

Figure 3.8. The Total Sediment Thickness map. Lines A, B, C, and D – composite lines used in this study; lines in red color – transects from Marton et al., (2005); lines in black between 5°S and 9°S – profiles from Contrucci et al., (2004) and Moulin et al., (2005).

Age	Generalized lithology of stratigraphic units of Marton et al., (2000)	Interval velocity (km/s)	Density from Fig.9, (g/cm3)	Densities of the stratigraphic units used in this work, (g/cm3)
Pliocene to recent	sandstone	2.1	2.0	2.05 - 2.2
Miocene	silt/sandstone	2.3	2.05	2.1 – 2.25
Albian to top Oligocene	carbonates, sandstones	3.2 – 3.4	2.2 – 2.25	2.2 – 2.35
Aptian	salt	4.5		2.2
Barremian to Early Aptian	sandstone, shale, siltstone of the pre-salt wedge	4	2.35	2.5
Late Jurassic-Early Cretaceous	shale, sandstone of the syn-rift section	4.2	2.4	2.55
Precambrian	basement	5	2.7	2.85 (oceanic crust)
				2.8 (continental crust)
				3.2 (mantle)

Table 3.1. Stratigraphic units from Marton et al., (2000) and of this work, and their average densities.

Lithology	Density range	Density average
Basic Igneous	2.09 - 3.17	2.79
Metamorphic	2.40 - 3.10	2.74
Dolomite	2.36 - 2.90	2.70
Acid Igneous	2.30 - 3.11	2.61
Limestone	1 .93 - 2.90	2.54
Shale	1.77 - 2.45	2.42
Sandstone	1.61 - 2.76	2.32

Table 3.2. Rock densities, modified from Dobrin and Savit (1988).

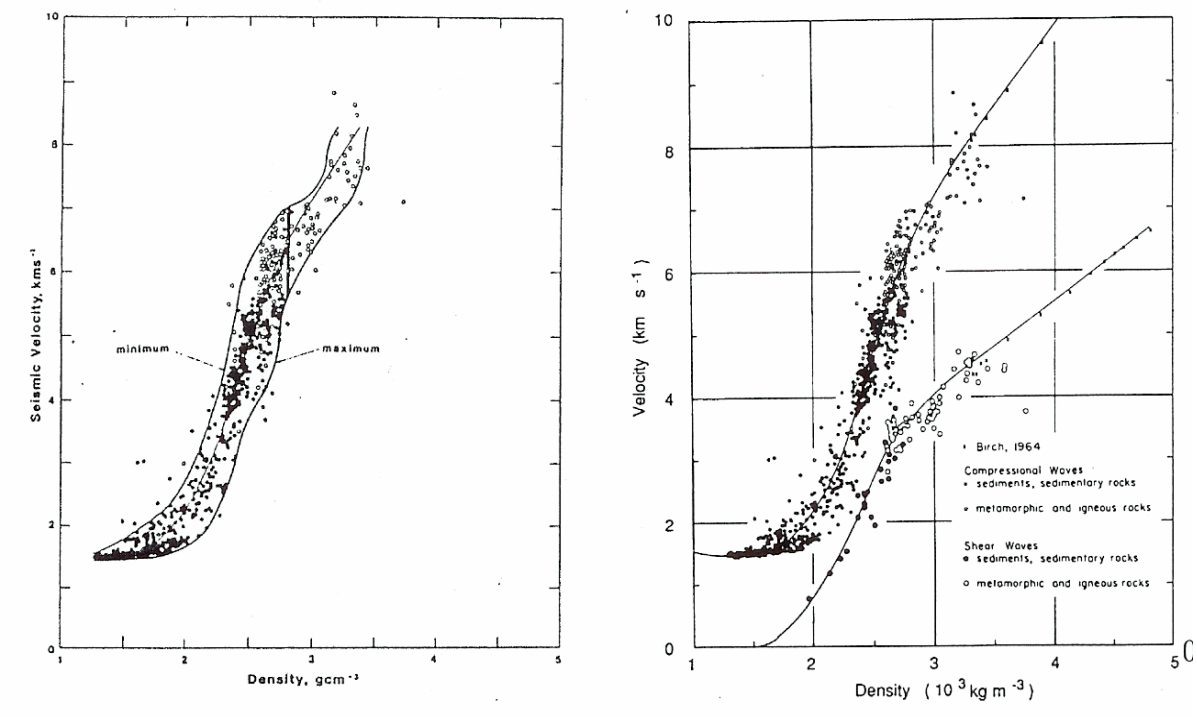

Figure 3.9. Density vs seismic velocity.

4. RESULTS

4.1 Continent- ocean boundary

The location of the continent-ocean boundary (COB) was one of the targets in the crustal modelling during this work. To locate the COB, the potential field gradient was evaluated. The Bouguer gravity anomaly has proved particularly useful in delineating the COB. (Karner & Driscoll, 1999). Generally, the COB is defined by the highest gradient in the Bouguer gravity anomaly reflecting the shallowing of Moho from the continent to the oceanic side. To calculate the Bouguer gravity anomaly bathymetry-gravity data along ship-borne tracks and from gridded data along chosen azimuths were extracted. This work has been done for the composite lines A, B, C, and D by means of GMT (Fig. 4.1). Ship-borne data along the lines were utilized where they were available, while elsewhere gridded data were used. Due to the limited availability of high resolution ship-borne data, the following scheme was used for the extraction of gravity and bathymetry data along the four transects:

- Line A – fully composed of gridded data.
- Line B - for the first 202 km (considering that starting point is the extreme west point) gridded data were utilized, than data from track ivk01, from 13140 km to 13345 km, and track a2677, from 60km to 206km, were added.
- Line C – fully composed of gridded data.
- Line D – fully composed of gridded data.

For comparison, similar data were extracted along track a2676, from 3160 km to 3750 km. This part of track a2676 is located close to Line D and is located almost parallel to it. Due to rapid lateral changes in lithologies and structure within the study area, the gridded data were used in further modelling of Line D. Ship-borne magnetic data were extracted along tracks as well. Furthermore, the calculated Bouguer corrected anomalies, gravity anomalies and bathymetry curves were plotted in one plot. Magnetic data, when available, were plotted in the same plots. Figure 4.1 represents the outcome of this stage.

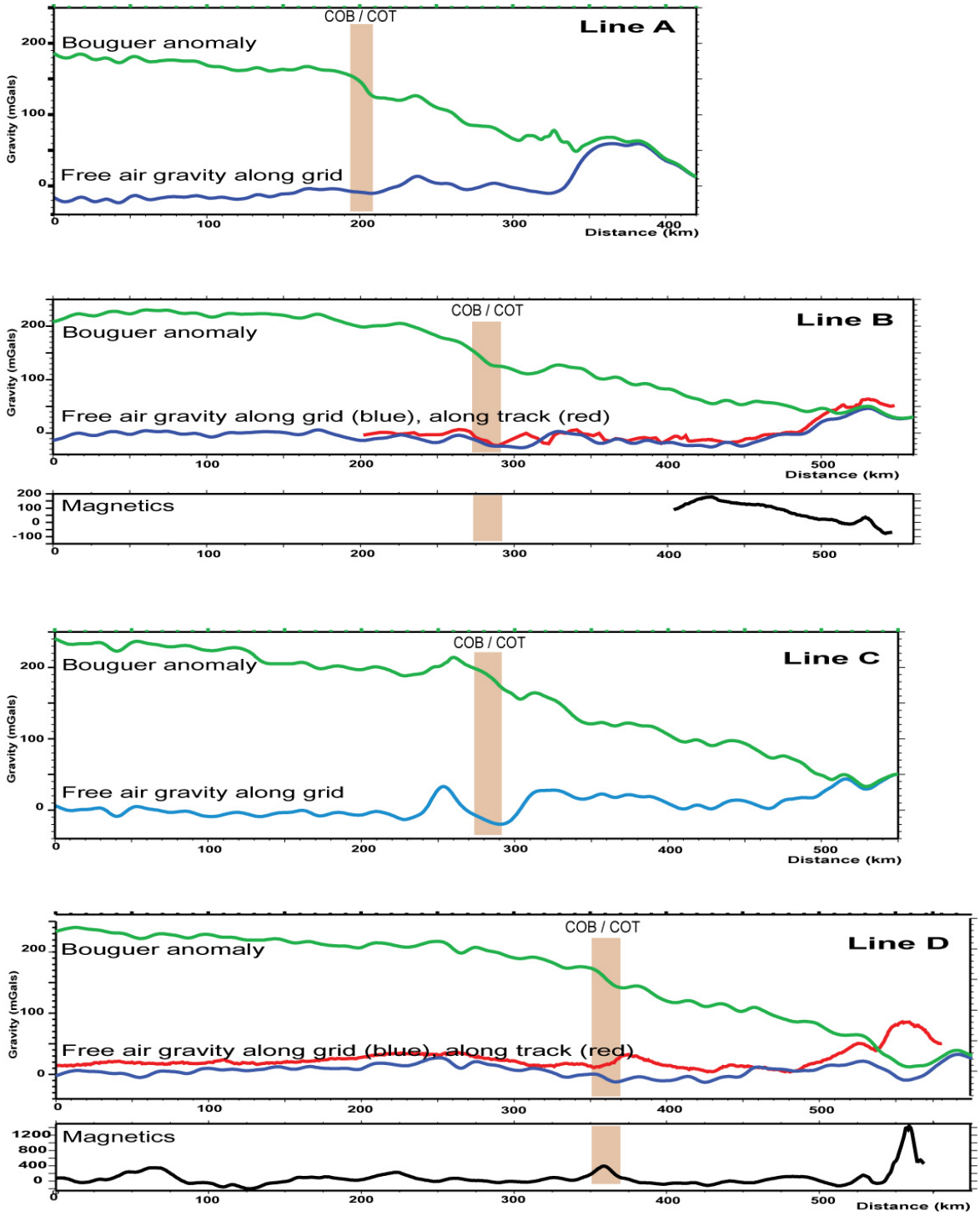

Figure 4.1. Gravity anomaly, Bouguer anomaly, magnetics extracted from gridded data and along tracks. Lines A, B, C and D.

4.2 Moho relief

Another essential part in the crustal modelling of this work was the definition of Moho geometries. The methodologies for constructing Moho geometries include forward and inverse gravity modeling of a simplified crustal model. The in-house software *TAMP* was utilized for these purposes.

Generally *forward modeling* involves creating a hypothetical geologic model that would fit available information about geology of the area. *Inverse modeling* in this study was aimed to adjust the Moho relief through several iterations by minimizing the discrepancy between the calculated and observed gravity values.

In forward and inverse modelling the earth model is simplified to have been represented by 3 polygons: water, crust and mantle. The input parameters include average density values for these polygons. The density values for water and mantle were accepted as 1.03 g/cm^3 and 3.2 g/cm^3. For the crustal densities different values ranging from 2.70 g/cm^3 to 2.90 g/cm^3 have been tried through several runs. Bathymetry, extracted from grid, observed gravity data, extracted from tracks or grid, and the anchor-point – the constraint for Moho-depth (the global average value for oceanic crust = 6.5 km) - were the additional input data set.

The outcome of gravity forward modelling is the isostatically balanced Moho relief (Fig. 4.2). In inverse modelling the input data is the same as in forward modeling. In addition the input data included planar initial Moho surface. The outcome was the iteratively adjusted Moho relief. In inverse modeling the whole transect is divided into blocks within each of which the Moho depth is calculated through several iterations. It is the task of the user to define the reasonable values for the blocks width and number of iterations. As a result of many runs the optimal width of the blocks was considered to be 20 km and the optimal number of iterations was considered to be within ranges from 5 to 10. Increasing the number of iterations increases the picks, making the trend more visible. Hence if the overall trend within the block or few blocks is to increase the Moho depth, then increasing value of iterations will increase the Moho depths even more.

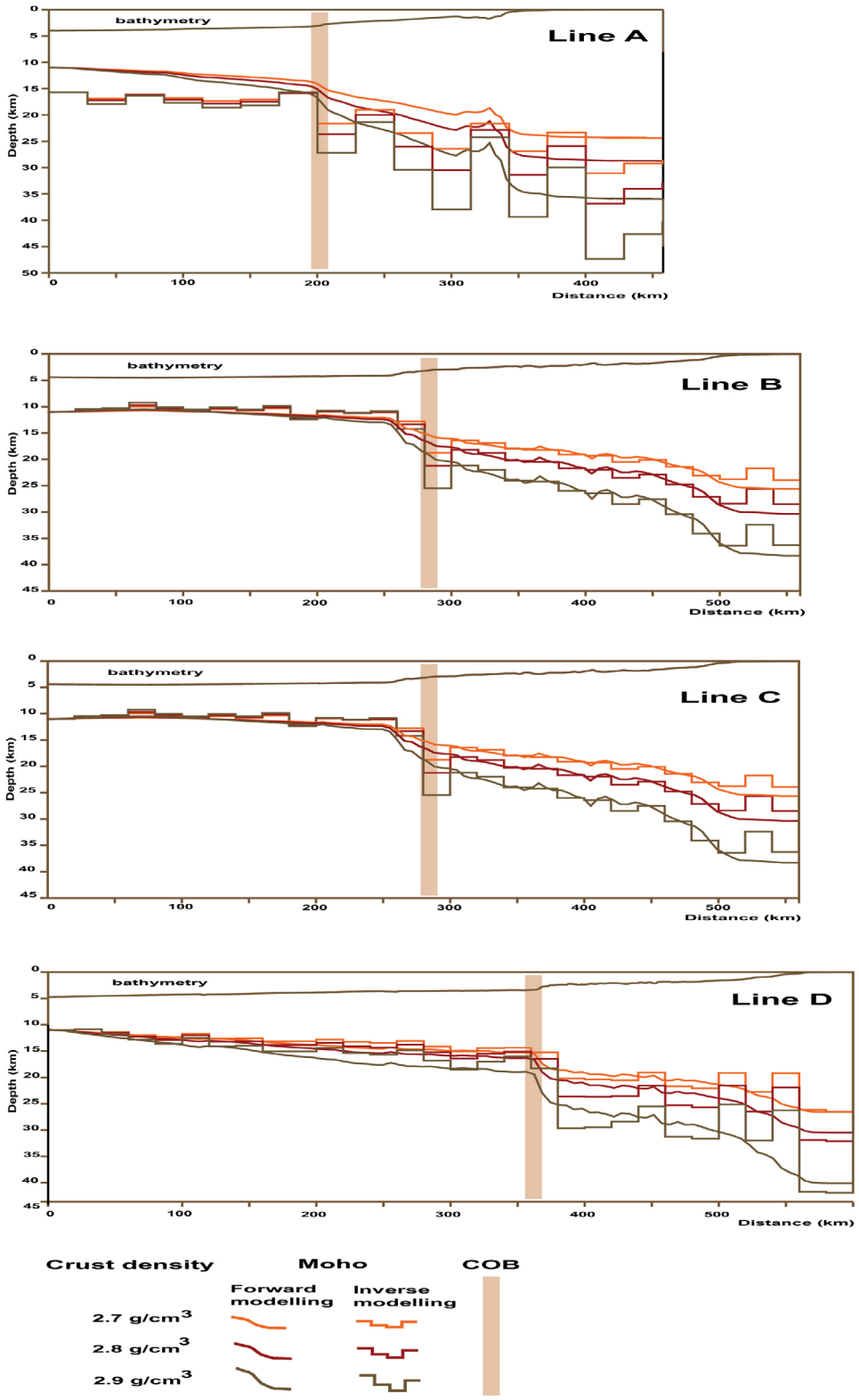

Figure 4.2. Moho relief defined by forward and inverse modelling. Lines A, B, C and D.

Number of iterations ranging from 5 to 10 was considered as giving the most stable and robust results. According to methodology of forward and inverse gravity modeling with TAMP it is reasonable to “smooth” extensively the output of the inverse modelling as the latter is aimed to verify the results of the forward modelling. It is the forward modelling/isostatic balance that is the most reliable method to obtain the first order approximation for Moho relief.

Figure 4.2 represents the outcome of the forward (smooth lines) and inverse (stepwise lines) modeling for lines A, B, C, D. The red color represent the outcome for crustal densities 2.7 g/cm^3, blue color stands for the density values of 2.8 g/cm^3, while black color assigned to the outcome for crustal densities of 2.9 g/cm^3. Bathymetry was plotted on the same plots (smooth line in black color above the Moho-lines).

4.3 Gravity modelling, - crustal transects

As it was mentioned above, by means of the software TAMP a first order approximation of the Moho depth was obtained. Interactive 2D gravity modelling was performed with the GM-SYS software (Northwest Geophysical Associates, Inc.) by detailed iterative fit of both the long- and mostly the short-wavelength gravity anomalies along the selected profiles. Gravity modelling carries on the aspect of “non-uniqueness”; i.e. several earth models can produce the same gravity anomaly response. Therefore, the final result depends on how reasonable the starting model and the regional considerations are, as well as the systematic and well-justified modelling steps. The input data for 2D gravity modelling includes the two-dimensional flat-earth model, typical densities for stratigraphic units represented within the earth model, and observed values for gravity within the earth model.

A two-dimensional earth model was created for each line. The Moho-level outcome of the forward modelling from TAMP (Fig. 4.2), together with bathymetry along each line was overlain by accurately scaled transects from Marton et al. (2000) (Fig. 3.2). The bathymetric data included in the resulting plots from the TAMP-modelling were extracted from grid, so it was assumed reasonable to make small adjustments in the transect locations. For Line D two earth models were

created: one with the transect D from Marton et al. (2000) (Fig. 4.6) as a background, and another with profile G from Gjelberg & Valle (2003) (Fig. 4.7). Despite transect D from Marton et al. (2000) and profile G from Gjelberg & Valle (2003) have the same location (Fig. 4.8), they differ in terms of top-basement and top-salt depths. Most likely this is due to differences in seismic velocities used for depth conversion. The seaward extension of each line was constructed by means of the sediment thickness map (Fig. 3.8). From this map, the thickness of the sedimentary sequences in the abyssal part was obtained and taken into consideration with certain precautions. The reason for precautions is that the data values in the digital total sediment thickness database for the world's oceans and marginal seas represent the depth to acoustic basement. The acoustic basement may not actually represent the base of the sediments. These data are intended to provide a minimum value for the thickness of the sediment in a particular geographic region.

Several intervals were differentiated and average density values were assigned (Table 3.1). The densities used in this work were derived from the Nafe & Drake empirical velocity-density relationship (Nafe & Drake, 1957; Ludwig et al., 1970) (Fig. 3.9). The chosen density values were compared with values given by Dobrin and Savit (1988) (Table 3.2.). The density values used in this work mostly belong to the upper part of the range from Table 3.2. Such values were chosen with regard to considerable age and depths of the rocks. Furthermore, lateral variations in densities within the sedimentary units were introduced to better fit the discrepancies between the calculated and observed gravity anomalies. The main aspects of the lateral density variation are the following:

1. The sedimentary units have lower density values within the oceanic part compared to the continental part. This can be explained by the lower rates of compaction within oceanic part of the lines.
2. Upwards to the shelf the density values are changing to the lower numbers for the same sedimentary units. This has been done with regard to higher rates of compaction within larger depths.
3. The density values for the sequences within the sedimentary fans, namely the Lower Congo Fan (Line A, Figure 4.3) and the Kwanza Fan (Line C, Figure 4.5), were changed to slightly higher numbers with regard to higher rates of compaction.

Furthermore, considering the higher diversity in density values due to salt tectonics-related high geometries within the sedimentary succession in continental part, the whole succession was separated into three units - Albian to top Oligocene, Miocene, and Pliocene to recent (Table 3.1). For the oceanic part Albian to top Oligocene and Miocene were joined to one unit.

The first step taken in gravity modelling was to determine if there was a regional trend in the observed gravity anomaly data, reflecting a regional long-wavelength anomaly related to deep-seated features within the crust. At this step the adjustments concerned mostly the geometries of Moho and the crustal structure of the model. The second step was to determine if the short-wavelength gravity anomalies could be approximated by a shape of tilted blocks or faults juxtaposing sedimentary sequences with different densities. At this step, the adjustments were made mostly for the boundaries below the salt layer. This is because the geometries above salt were obtained by detailed seismic interpretation and are considered reliable, not bearing further adjustments. On the contrary, the geometries below salt suffer from the low resolution of the seismic reflection data due to the masking effect of the salt layer. Hence, the contribution of gravity modelling is considerable in deciphering and imaging these deep geometries. The remaining discrepancies were adjusted partly by introducing a high-velocity/density Lower Crustal Body (Line A, Figure 4.3) and partly by introducing lateral density variations within the sedimentary units as explained above.

The outcome of the GM-SYS gravity modelling is presented on Figs. 4.3, 4.4, 4.5, 4.6, and 4.7. The gravity models form the basis for a set of regional crustal transects, that will be described and discussed in the next chapter.

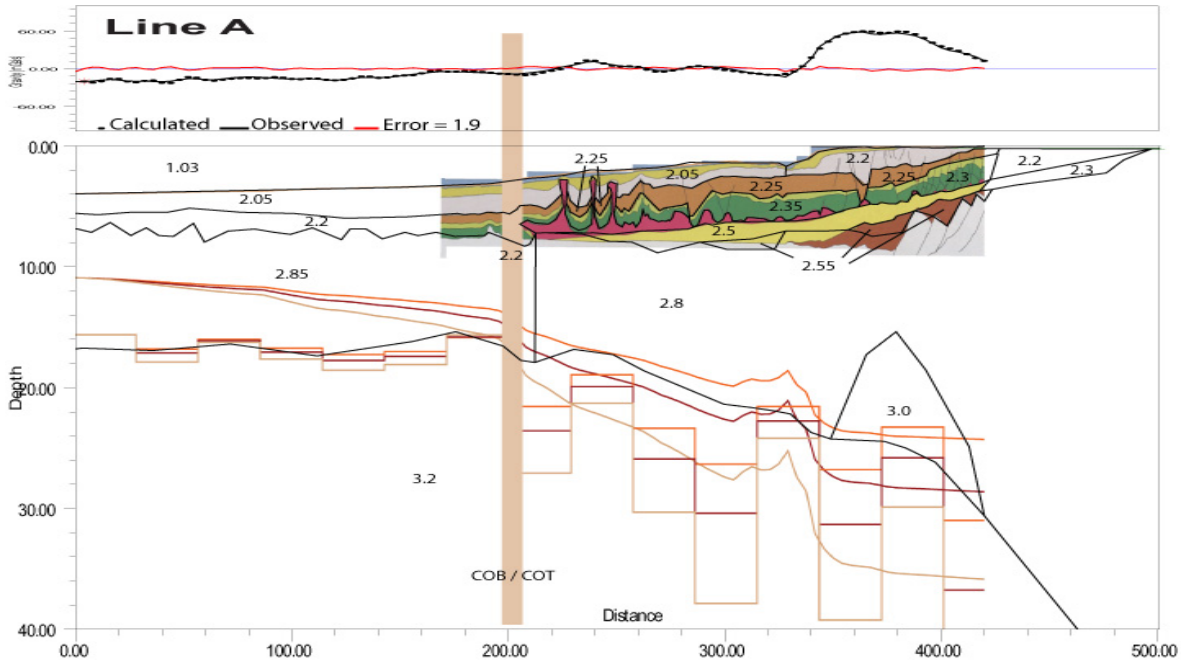

Figure 4.3. Gravity modelling, Line A. The background of continental part is transect A, Marton et al., 2000.

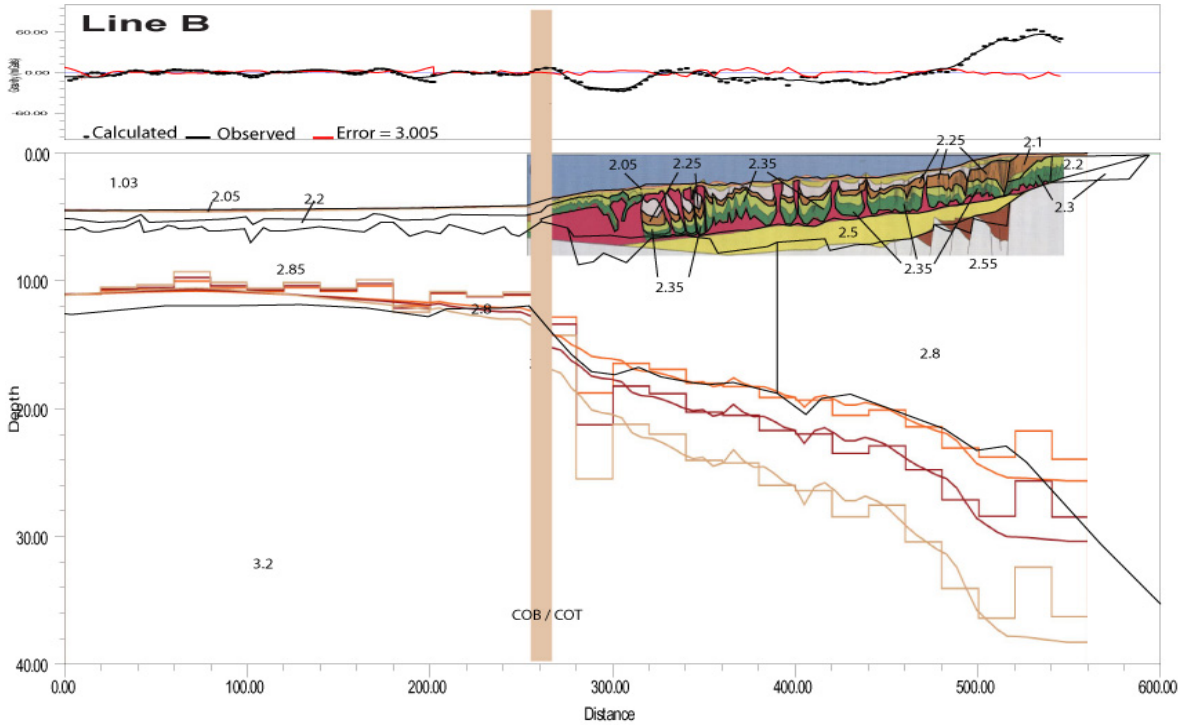

Figure 4.4. Gravity modelling, Line B. The background of continental part is transect B, Marton et al. 2000.

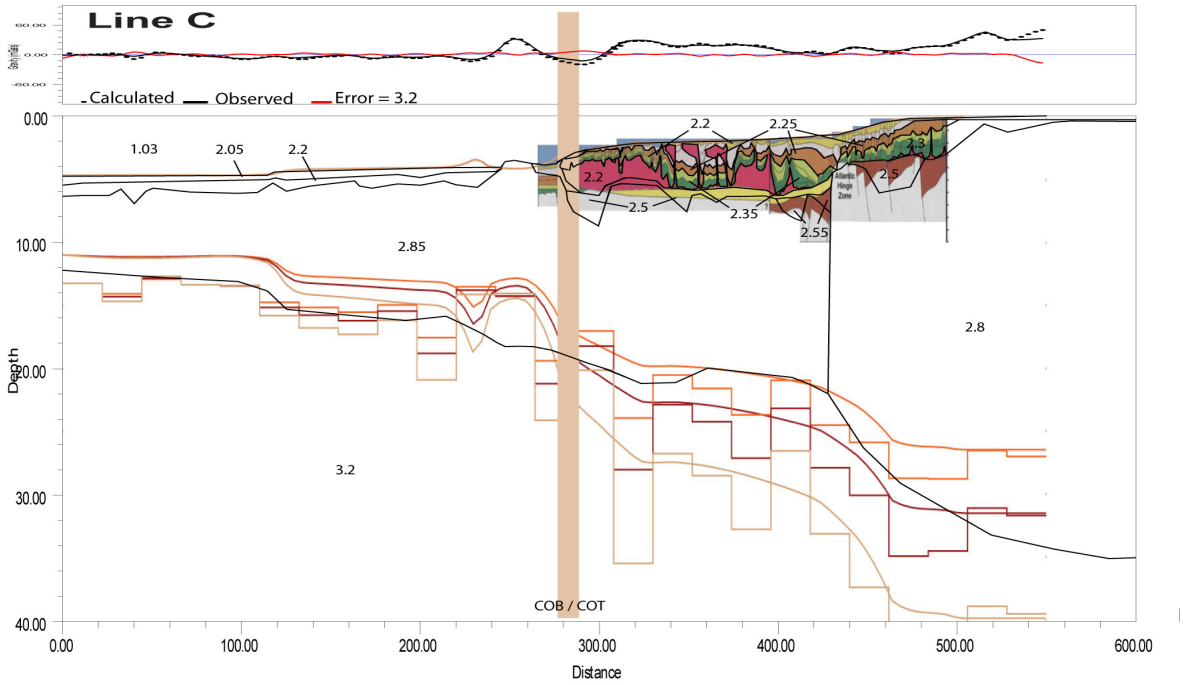

Figure 4.5. Gravity modelling, Line C. The background of continental part is transect C, Marton et al., 2000.

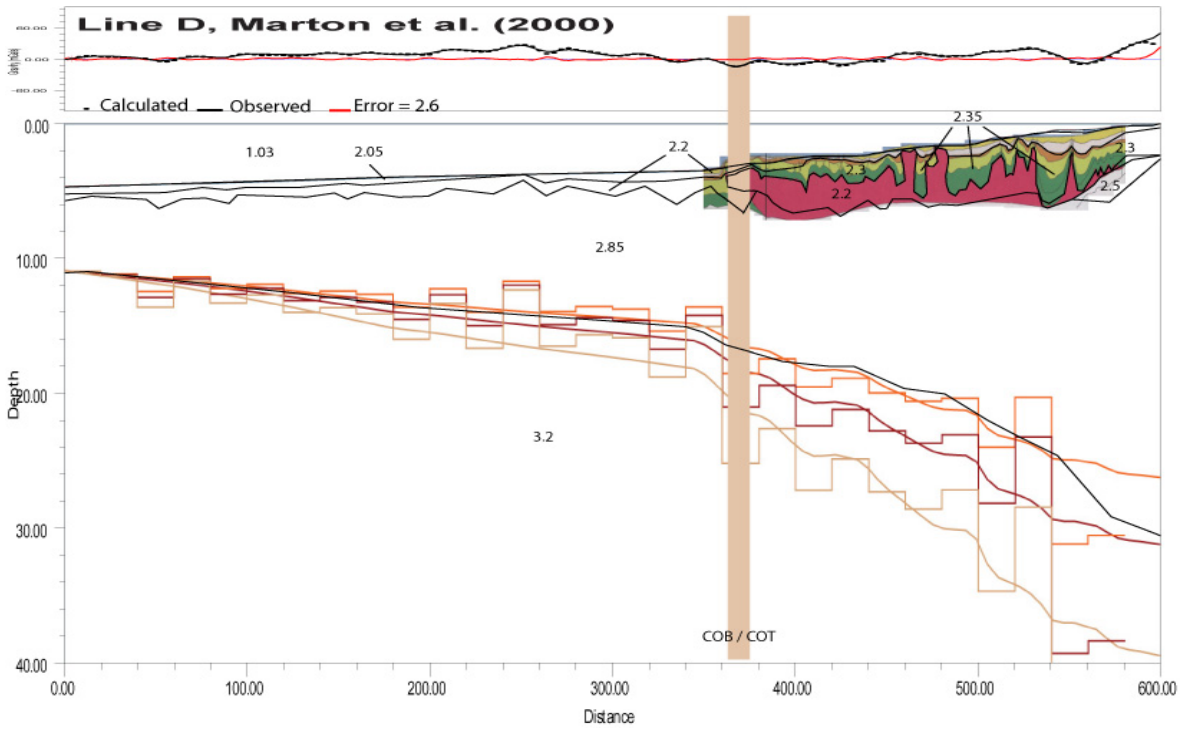

Figure 4.6. Gravity modelling, Line D. The background of continental part is transect D, Marton et al., 2000.

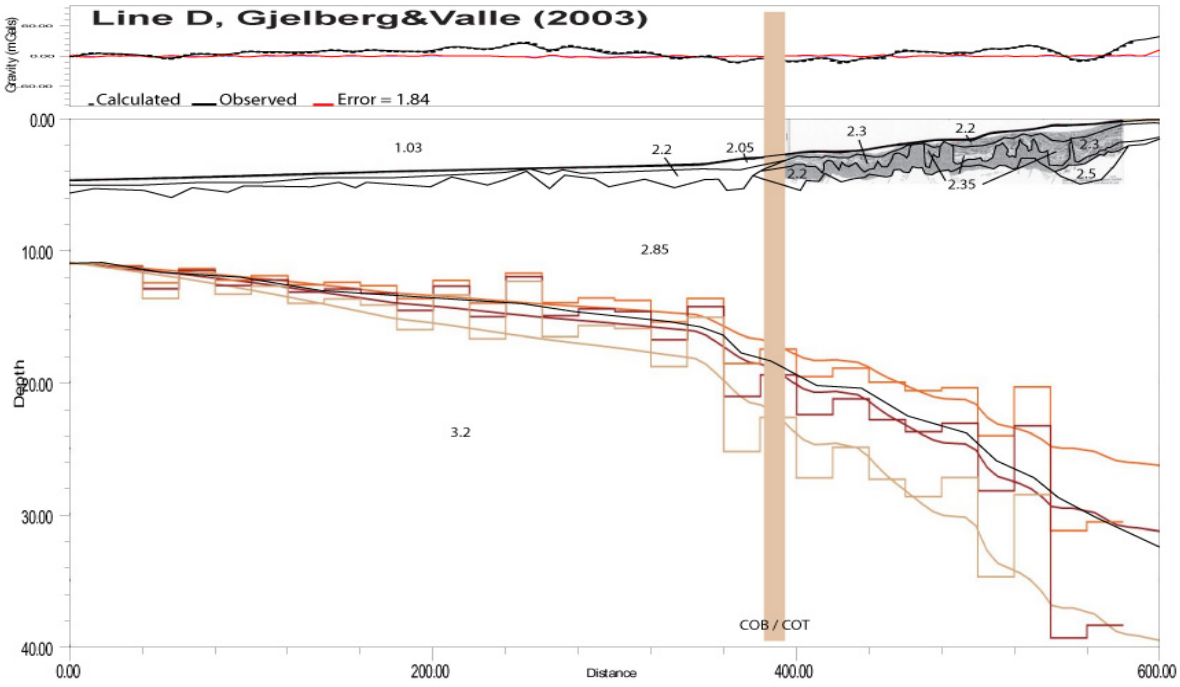

Figure 4.7. Gravity modelling, Line D. The background of continental part is profile G, Gjelberg & Valle (2003).

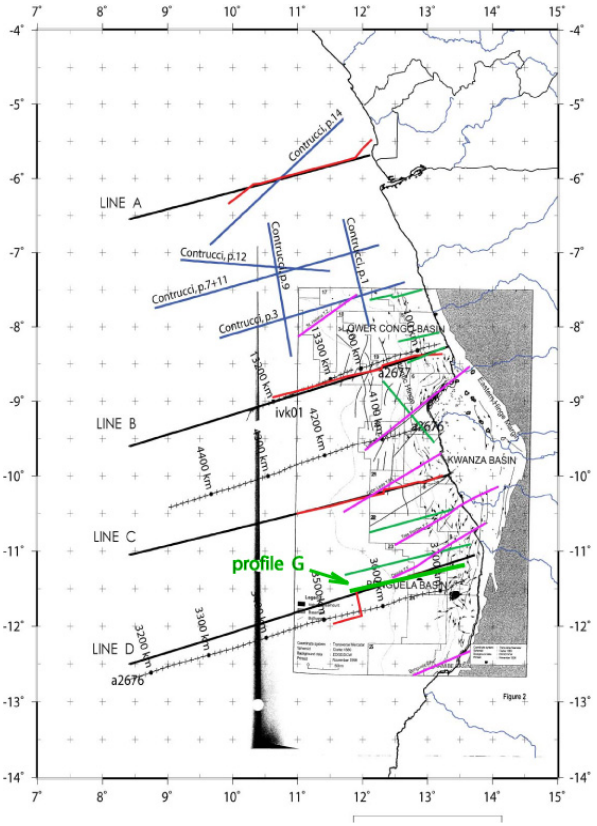

Figure 4.8. Study area with superposed seismic profiles and transfer zones from Gjelberg&Valle (2003).

5. DISCUSSION

5.1 Bathymetry and potential field features

The bathymetry map (Fig. 3.1) clearly reveals three sedimentary fans: the Lower Congo Basin in the northern part of the area, the Kwanza Basin in the centre and the Benguela Basin in the southern part of the area. The southern edge of the Dentale Basin fan is located in the north of the study area. The Congo Canyon reaches depths of almost 1000 m and cut the Lower Congo Basin Fan in an E-W direction, oblique to the coastline. The continental shelf, which edge can be outlined by 200-m-isobath, stretches almost parallel to the coastline, and is about 50 km wide in the north of the study area and almost diminishes in the south. The sedimentary fans extend seawards to about 200 km in the Lower Congo Basin and 150 km in the Kwanza Basin. Within the Benguela Basin, the shelf is narrowing to a width of 50 km in the middle of the basin and even less further on to the south.

The continental slope is steep and narrow in the northern part of the area and extends to about 200 km from the coastline. Within the sedimentary fans of the Lower Congo Basin and the Kwanza Basin the continental slope has significantly lower gradients and broadens to about 300–350 km for the Lower Congo Basin and 250 km for the Kwanza Basin. Southward, within the Benguela Basin, the continental slope has remarkably lesser width, and extends to about 150–200 km. The Kwanza volcanic line, that separates the Kwanza Basin and the Benguela Basin (Fig. 3.4), has evident impact on the distribution of the sediments within its vicinity. Northwards of the volcanic line, the sedimentary fan is much broader and extends far seaward in comparison to the sedimentary fan southward of the volcanic line. The bathymetric highs of the volcanic line have probably acted as a barrier for the sediment transport in the SW direction. The abyssal plain within the study area reaches depths of about 4000–5000 m and uniformly deepens seaward.

The most distinctive feature of the free-air gravity map (Fig. 5.1, a) is the “edge effect”. The edge effect gravity anomaly has been interpreted in terms of geological processes that are related to the crustal structure of the margin (Walcott, 1972; Watts, 1988), such as sedimentation and magmatism. This gravity anomaly consists of a gravity high near the shelf break and a gravity low over the continental slope (Stewart et al., 2000). Within the study area the edge effect anomaly signature is rather complex and clearly divides the margin into two

a)

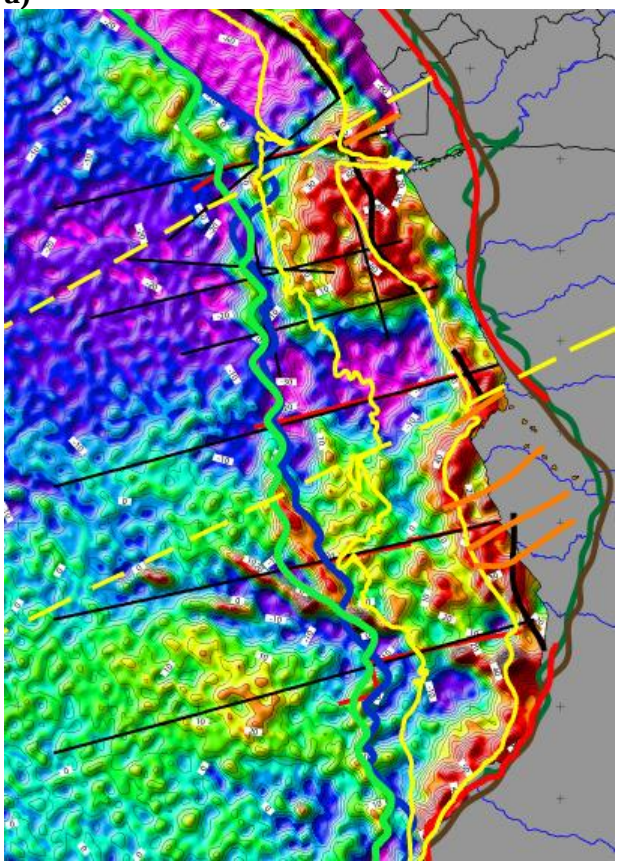

b)

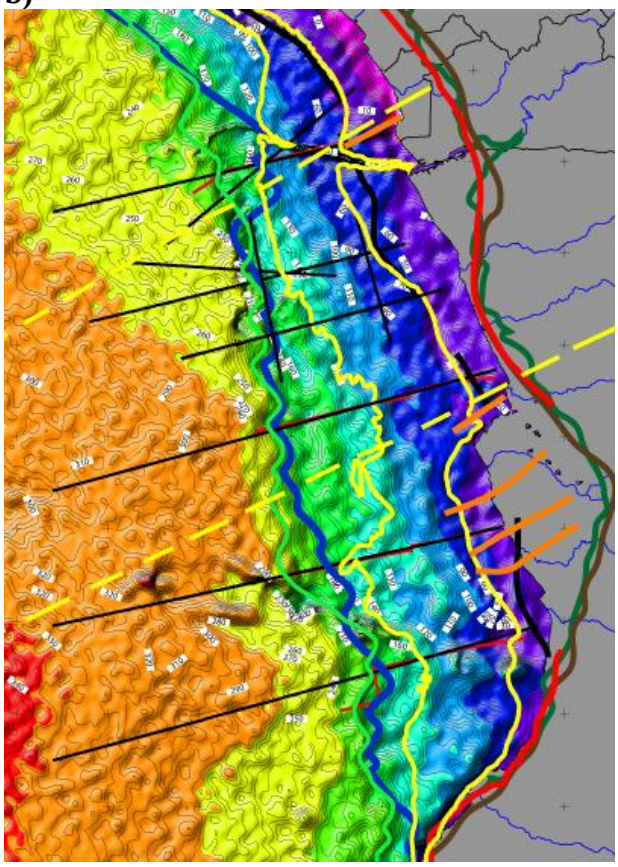

c)

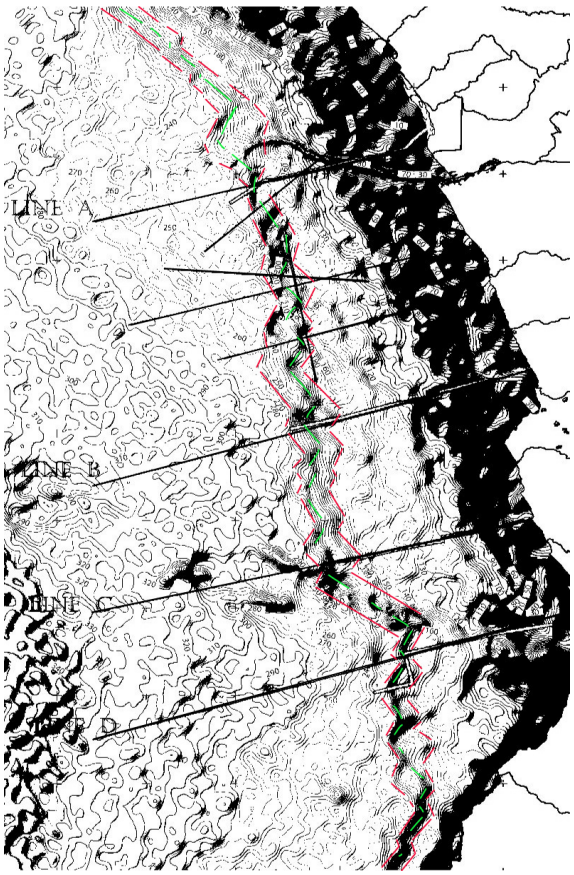

Figure 5.1. a) Free-air gravity anomaly map; b) Bouguer gravity map; c) The image of the Bouguer map created in GIMP (a freely distributed GNU Image Manipulation Program; www.gimp.com).
Illustrated on a) and b) are: COB defined in this work (light green), COB from Karner & Driscoll (1999) (blue), isobaths 200 m and 2000 m (yellow); the Atlantic Hinge (black) and the Eastern Hinge (red) from Karner & Driscoll (1999); the boundary of onshore basins (brown) (Davison, 1999; Marton et al. 2000); the contour line delineating lowland (dark green); the transfer zones (orange) (Hudec & Jackson, 2002; Figueiredo & Murthy, 2002); the boundaries between segments and compartments (dashed yellow). Thin black and red lines - lines A, B, C, D, transects from Marton et al. (2000) and profiles from Contrucci et al. (2004).
Illustrated on c) are: boundaries of the zone with the high gradient in Bouguergravity anomaly (red); COB (green).

segments. The northern segment is characterized with “lows” landward and seaward of the gravity high. The “high”-“low” trend in the northern segment is interrupted by the Lower Congo Fan. To the north of the Lower Congo Fan the landward and seaward “lows” are prominent and may possibly be related to a distinct regional-scale feature in the crustal structure. Offshore Gabon, this feature was interpreted by Watts & Stewart (1998) to represent a weak segment of the lithosphere. The western flank of the “lithosphere”-related low is marked by a new “high”, that along with the high on the eastern flank can be related to a thick sedimentary sequence of a southern edge of the Gabon Basin (Fig. 3.8). To the south of the Lower Congo Fan, the seaward low continues while the landward low is fading out. The southern margin segment within the study area does not reveal the landward low while the seaward low can be traced until it is being interrupted by the Kwanza volcanic line.

Furthermore, the two margin segments have different signatures in the abyssal-plain part, where the northern segment is characterised by overall low gravity values, while the southern segment has significantly higher values. The gravity signature of the Kwanza volcanic line can be characterized with the “high” along the northern side of the volcanic line and the “low” along the southern side of the line. Watts & Stewart (1998) explained the “high”–“low” trend to be associated with sedimentation resulting in a positive contribution due to the sediment load and a negative contribution from the flexure of the basement and the underlying Moho. The highs reflect the magnitude of the sediment load while the lows are indicative of the degree to which the load is compensated. The same agreement may be applied to the “high”–“low” trend along the volcanic line where the load is of volcanic origin. The gravity signature of the volcanic line reveals two northward-stretching branches that start from the main line approximately where it crosses the 12° E longitude. The two branches stretch almost parallel to the coastline.

While the gravity signature of the southern segment is relatively simple, the signature of the northern segment suggests further division into two provinces. The border between the provinces separating the Lower Congo Fan from the Gabon Basin, is oriented ENE–WSW. The province, to which the Lower Congo Basin belongs, has no prominent gravity lows close to the coastline and exhibits, in overall, higher amplitude gravity anomalies in comparison to the other one.

The continent-ocean boundary (COB) has been delineated close to the strong positive-negative gradient on the Bouguer gravity anomaly map (Figures 3.6 and 5.1, b). The GIMP-image was useful in defining the zone with high gradient in Bouguer anomaly across the margin (Fig. 5.1, c). Within the study area the COB stretches almost along the coastline in a NNW–SSE direction until approximately 12° S. At this latitude the coastline changes its direction westward while the COB continues in the same direction. Southwards, the COB comes close to the coastline and from 13° S it stretches along the coastline. Both the free-air and the Bouguer-corrected gravity anomaly profiles along the extracted azimuths from grid and ship-borne data were particularly useful in defining the cross-points of COB with the published profiles of Marton et al. (2000). As the transition from continental to oceanic crust takes place within a zone with a nominal width, the parts of the Bouguer gravity anomaly with the high gradient were delineated on each of them. Within this part on each profile the point was chosen where the gradient was considered to be the highest to represent the COB reflecting the shallowing of Moho from the continental to the oceanic domain. These points consequently were the main constraints in delineating the COB within the study area. The resultant COB was compared with the COB of Karner & Driscoll (1999). The greatest misfit is about 25 km and is located where two boundaries are crossing Line A. As the COB location within this line was confirmed by the gridded and ship-borne data, the methodology is proven to be very robust and the mapped COB location was used in the subsequent analysis. Another essential misfit is about 20 km and is located in the vicinity of the volcanic line, in its northward stretching branch. The Bouguer gravity anomaly here is strongly affected by the load of the intruded material, so some deviation in the COB location is to be expected.

The geometry of the COB reflects the two main types of tectonically induced horizontal movements, which are movements due to extension and due to shear motion. The COB is represented by a line which can be generally divided into two types of segments, one along the strike of the coastline and another perpendicular or almost perpendicular to the strike of the coastline. The segments of the second type that are considerably shorter than that of the first type, are considered to result from strike-slip or shear induced offsets in the COB.

That was noticed by several authors that the transition from oceanic domain to continental domain is coincident with the outer high in the basement top. Spathopoulos (1996) explained the location of the westward edge of the salt basin by the existence of a basement or volcanic high that acts as a fixed point against which all compression must be accommodated. Meyers

et al. (1996) described the closely spaced, faulted crustal structures associated with magnetic anomalies, to resemble outer highs. These outer highs were interpreted as faulted, mafic volcanic blocks resting above or intermixed with remnants of thinned and possibly detached slivers of continental crust. Similar basement ridges have been described along the outer margins of the Angola Basin. The origin of these highs is debated and has been related to uplifted continental crust or to be completely oceanic crust. The presence of a basement ridge was clearly documented on studies in the Lower Congo Basin (Contrucci et al., 2004; Moulin et al., 2005). The transitional zone is bounded to the west by a basement ridge. This basement ridge is located below the western end of the salt compressive front. In this work the outer high was defined in lines A, B, and C. Within line A it is not possible to identify on basis of this work the nature of the outer high, while within lines B and C the outer high clearly reveals volcanic nature.

Additional structural features within the study area were particularly revealed by the magnetic anomaly map (Fig. 3.7). It is possible to trace the Kwanza volcanic line on this map, which shows that the northward stretching branches of it are extending quite far to the north, reaching the area of the Lower Congo Fan and possibly further on towards the gravity low within the Gabon Basin. Furthermore, segmentation of the study area is clearly revealed by 2D gravity modelling (Fig. 5.2). The resulting gravity models for the four studied lines substantiate the complex margin crustal structure and subsequently its impact on the sediment distribution.

5.2 Margin architecture

Line A

Line A (Figures 4.12 and 5.2) has the thickest sedimentary sequence in the abyssal part compared to the other lines. The basement top here is approximately at 7 km depth, varying within 6-8 km due to sea-floor spreading related disturbance. The considerably thick sedimentary package was related to the influence of the Congo Fan. Landwards, the sedimentary sequence thickens significantly within the thick subsalt basin and mostly within the Lower Congo Basin. Beneath the sedimentary sequences, the top-basement reflections reveal rift-related faulted geometries with tilted blocks rotated landward. Further landwards, the top-basement reflector is step-ward elevated, with each prominent rise being coincident with two hinges, the Atlantic Hinge and the Eastern Hinge (Karner & Driscoll, 1999). The

Moho lies at 17 km depth in the abyssal part and is slightly elevated in the middle of Line A. Moho uniformly deepens landwards and rapidly reaches down to 40 km close to the mainland. The significant gravity high in the landward part of Line A was partly related to the density variations in the sedimentary succession and partly to the presence of the high-velocity (7+ km/s) Lower Crustal Body (LCB). The introduction of a LCB within Line A, coinciding with the prominent gravity high, is consistent with the results of other relevant studies (Contrucci et al., 2004; Moulin et al., 2005) (Fig. 2.9).

The oceanic crust is about 10 km thick and is thickest within Line A in comparison to the other lines. Landward from the COB the crust thickens almost uniformly, with the two distinctive step-like falls in Moho, each of which is coincident with basement top uplifts. One is located about 120 km landward from COB and in addition is coincident with the Congo River Canyon, and the other is located beneath the Atlantic Hinge (Fig. 5.2). The notable coincidence of the three features - the step-like fall in Moho, the basement top uplift and the Congo River Canyon that is attributed to a fault (Cramez & Jackson, 2000), proposes a deep fault, probably a transfer zone. Landward of the Atlantic Hinge the continental crust thickens abruptly to 35 km below the coastline. Landward of the Eastern Hinge the thickness of the crust was estimated to be generally more than 40 km. Within Line A, the continental crust exhibits a more or less uniform structure with a density of 2.8 g/cm^3. The seaward edge of the salt coincides with the outer high. The massive salt domain (Marton et al., 2000) has relatively small size and lies on top of the plateau formed by a large crustal block. The subsalt basin can be divided into two subbasins separated by a basement high; an interpretation that is also consistent with Moulin et al. (2005).

Line B

Line B (Figures 4.13 and 5.2) lies outside the extensive sedimentary fans and exhibits relatively thinner sedimentary sequences. Within the abyssal plain the thickness of the sediments is about 2 km. Towards the continent, the sedimentary thickness ranges from 6 km in the deepest parts of the basins to 2-3 km onshore Angola, and diminishes in the vicinity of the Eastern Hinge. The top-basement lies around a depth of 6 km in the oceanic part and exhibits high geometries due to sea-floor spreading. In the middle of Line B the top-basement is characterised by two prominent highs, that based on gravity and magnetic data analyses, were interpreted as the northward stretching branches of the Kwanza volcanic line. Further

landward within about 150 km, lies the zone of rift-related tilted blocks until the Atlantic Hinge gives a significant rise to the basement relief.

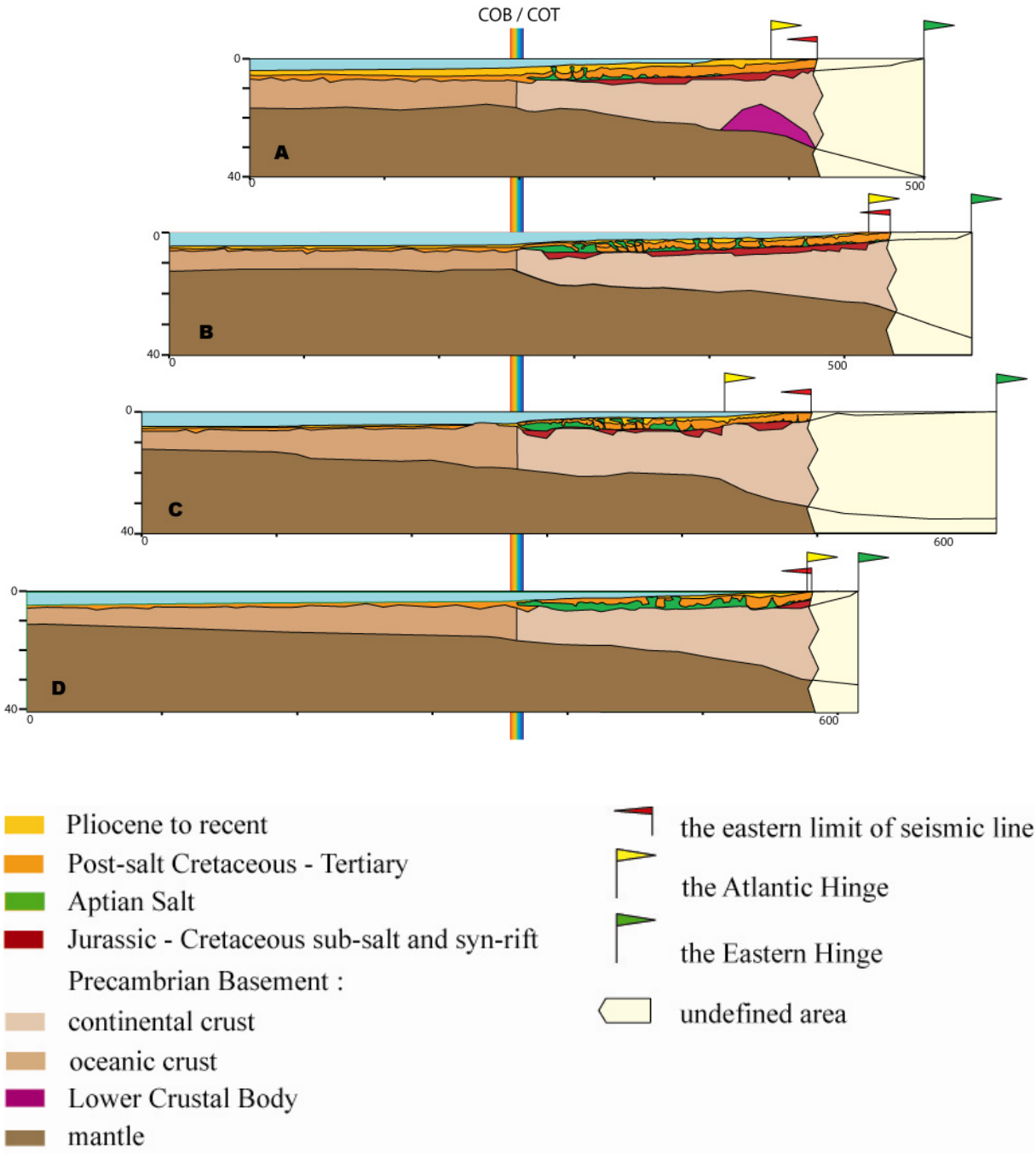

Figure 5.2. Crustal transects A, B, C, and D, based on seismic lines (Fig. 3.1) and gravity models (Figs. 4.3 – 4.6).

Moho within the abyssal plain is characterised by a smooth relief at depths of 11–12 km and a zone of prominent positive-negative gradient beneath the western branch of the volcanic line. Further landward within a distance of approximately 220 km, Moho lies at 18–22 km depth until a new zone of positive-negative gradient starts beneath the Atlantic Hinge. The oceanic crust is relatively thin and reaches a thickness of about 6 km. The continental crust has a thickness of 8 km on the seaward edge and thickens to about 18 km landward until the Atlantic Hinge. Further landward, the continental crust thickens rapidly to more than 35 km towards the Eastern Hinge. The continental crust along Line B exhibits a complex structure that is reflected by the modelled density variations. The part of the continental crust that lies within the first 100 km landward from the COB has a density of 2.85 g/cm^3. This relatively high average value for the crustal density can be accounted by a possible contribution from dense intruded magmatic material. Further on the crustal density changes to 2.8 g/cm^3. The subsalt basin can be divided to two small basins separated by the eastern branch of the Kwanza volcanic line. The eastern basin, in turn, can be further divided into two subbasins separated by a smooth basement-high similar within Line A. The massive salt domain covers the western subsalt basin and its seaward edge, and lies on top of the outer high.

Line C

Line C (Figures 4.14 and 5.2) is characterised by a thin sedimentary succession in the abyssal plain, exhibiting a thickness of ≥2 km. In its middle part, Line C crosses the Kwanza volcanic line, which represents a prominent bathymetric feature, namely the Kwanza seamounts. Landward of the seamounts, the sedimentary package thickens prominently. This suggests that the seamounts acted as a bathymetric barrier for sediment transport, as well as for the gravity induced salt movement seaward. The massive salt domain is roughly interrupted on its seaward edge by the wall of the seamounts. The relief of basement top appears complex, exhibiting a disturbed abyssal part, several seamounts, a zone of faulted and tilted blocks landwards of the seamounts, and two prominent stepward rises coincident with the two hinges, the Atlantic Hinge and the Eastern Hinge. Approximately beneath the coastline uplifted basement blocks are suggested that is consistent with other relevant studies (Hudec & Jackson, 2004). This basement high separates the outer offshore Kwanza Basin from the inner onshore Kwanza Basin. Moho deepens stepwise from a depth of 12 km in the western part of Line C, to approximately 21 km beneath the Atlantic Hinge; further landwards it deepens abruptly and reaches a 35 km depth beneath the onshore Kwanza Basin. The continental crust reveals a complex structure similar to Line B with densities changing landwards from 2.85

g/cm^3 to 2.80 g/cm^3. Transition from higher densities to lower is shifted landward relatively to Line B, while the COB is located almost at the same place as in Line B. A wide zone with high density coincides with the wide zone affected by intrusions. The subsalt sedimentary package is divided by volcanic highs and tilted crustal blocks to small basins that are probably not joined and were created independently from each other.

Line D

This line (Figures 4.15 and 5.2) exhibits overall shallower depths of the top-basement and Moho reflectors/levels in comparison to the other three lines. At the western end of the line, the top-basement lies at a depth of 6 km and Moho lies at a depth of 11 km. Landward, the top-basement becomes shallower and reaches a 5 km depth within 250 km from the western end. Farther landward, the top-basement reflector deepens slightly but still remains rather shallow in comparison to the previous lines. Overall along Line D, the top-basement reflector reveals rather highly structured, rift-related geometries.

Moho deepens gradually along Line D exhibiting a small gradient within the western half of the line and a higher gradient within the eastern half, and reaches depths of about 30 km at its eastern end. There is no density variation within the continental crust along Line D. That is possibly because the continental crust within Line D was intensively overprinted by magmatic activity. The contribution from the intruded material raised the average values of crustal density to 2.85 g/cm^3. It is worth noticing that the resultant model produced on the basis of profile G from Gjelberg & Valle (2003) gives deeper Moho levels for the continental crust (Fig. 4.16). The location of profile G is shown on Figure 4.17. The seismic data interpretation of Marton et al. (2000) differs from the interpretation of Gjelberg & Valle (2003) mostly in terms of the top-basement and top-salt depths. The top-basement and top-salt levels of Marton et al. (2000) are approximately 2 km deeper than that of Gjelberg & Valle (2003). That fact that different starting earth models consequently gave different results in GM-SYS is attributed to the "non-uniqueness" aspects of gravity modelling and was discussed in the "Data and Methods" chapter.

5.3 Margin segmentation

A distinct segmentation of the study area is clearly reflected in the potential field anomaly maps and gravity modelling results. In particular, the northern segment of the study area is

characterised by overall lower-amplitude gravity anomalies. Line A, located within the northern segment, reveals features that distinctly differentiate it from the other lines (Fig. 5.2). Line A exhibits a much deeper Moho compared to the other lines while the depths of the top-basement reflector are almost similar for all lines. Hence, the overall gravity anomalies within the northern segment are of lower amplitude due to the thicker crust. Line B crosses the border between the two segments while lines C and D belong to the southern segment of the study area. Comparing the abyssal part of Line B, which lies close to the southern segment, and the western parts of lines C and D, which are not affected by magmatic activity, it is possible to conclude that the overall high-amplitude gravity anomalies within the southern segment can be explained in terms of the thinner oceanic and continental crust and hence shallower Moho. While the LCB is present only in the northern segment of the study area, the volcanic activity has left a significant imprint on the southern part of the study area where the crust is thickened in isostatic response to the volcanic load. Furthermore, the sedimentary sequences exhibit the greatest thickness within Line A. This is in accordance with the "Total Sediment Thickness of the World's Oceans & Marginal Seas" showing that greater sediment thickness is a characteristic feature of the northern segment (Figure 3.7). Further subdivision of the northern segment into two provinces places Line A across the boundary between these provinces, where the cross point of Line A and the boundary is coincident with the cross point of Line A and COB. Therefore, the western part of Line A is located within the oceanic crust and the northern province, while the eastern part of Line A is located within the continental crust and the southern province. With this location of the line A it seems difficult to make any conclusions regarding the two provinces on the basis of the gravity modelling or the crustal structure is not affected by the further segmentation of the northern segment.

The onshore topography reveals a prominent consistency with the margin segmentation proposed on the basis of potential field analysis and gravity modelling within the study area (Fig. 5.3). The onshore counterpart of the northern segment is characterised by a lowland region extending farther eastward within the mainland, while the counterpart of the southern segment is characterised by a significantly uplifted area. The boundary between the lowland and highland is the onshore continuation of the boundary between the two offshore segments. The large-scale segmentation may be attributed to plate-tectonic processes. On the basis of several relevant studies (Davison, 1999; Hudec & Jackson, 2002; Figueiredo & Murthy, 2002; Mohriak & Rosendahl, 2002; Gjelberg & Valle, 2003; Hudec & Jackson, 2004) it is possible to postulate that the mainland to the east of the northern segment is occupied by the Congo–

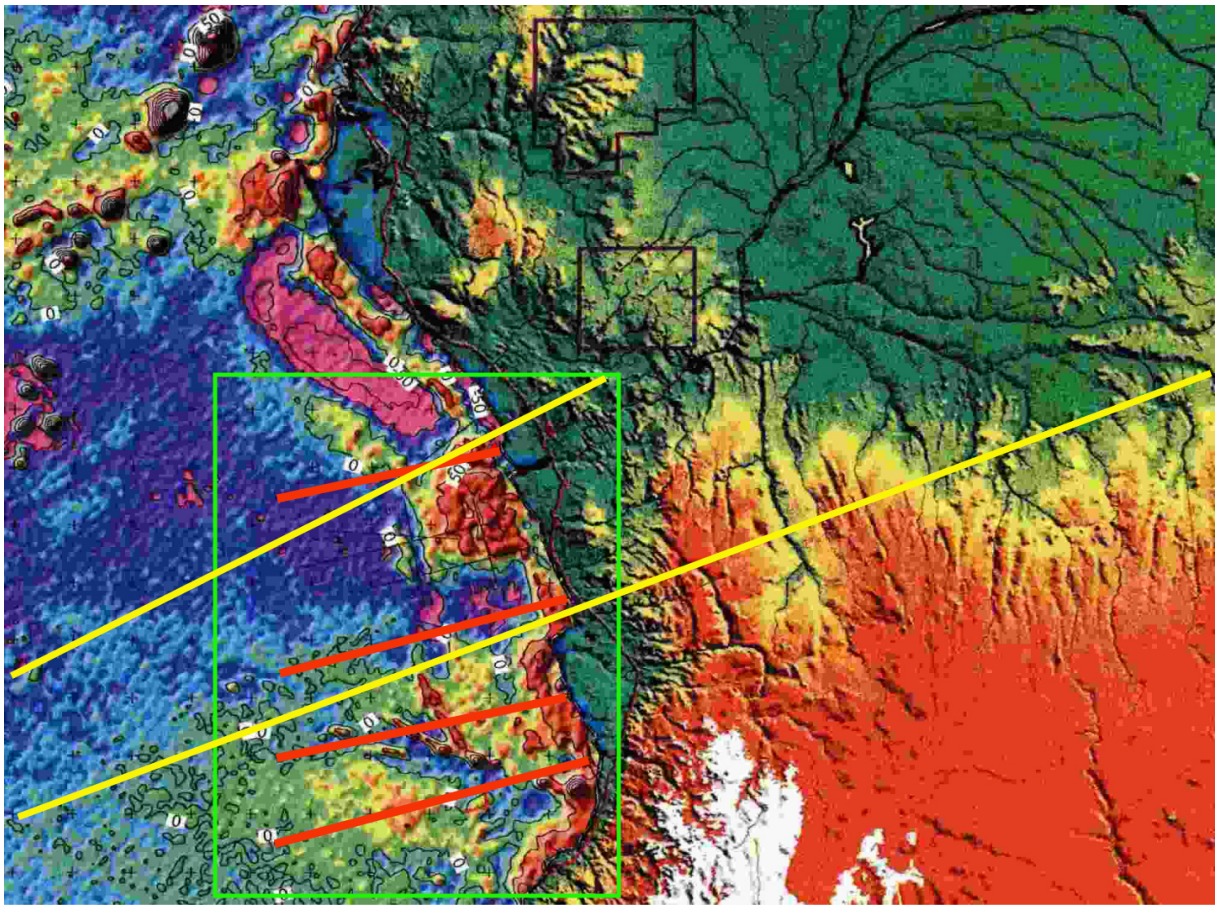

Figure 5.3. Onshore topography from Karner & Driscoll (1999) and offshore free-air gravity anomalies. Lines A, B, C, and D are in red, the borders between segments and compartments are in yellow.

Zair Craton, while to the east of the southern segments lies the Congo Fold Belt (Figures 5.4 and 5.5). Beyond the southern boundary of the study area lies the African superswell. That fact that the thicker crust within the northern segment correlates with the craton onshore, while the thinner crust of the southern segment, intensively affected by volcanism, correlates with the fold belt onshore, may not be purely coincidental.

The LCB is present only within the northern segment. Lower crustal bodies are found on many passive margins. The nature of lower crustal bodies is explained in terms of magmatic underplating, in particular volcanic settings, or high grade metamorphic rocks of earlier orogens (fold belts).

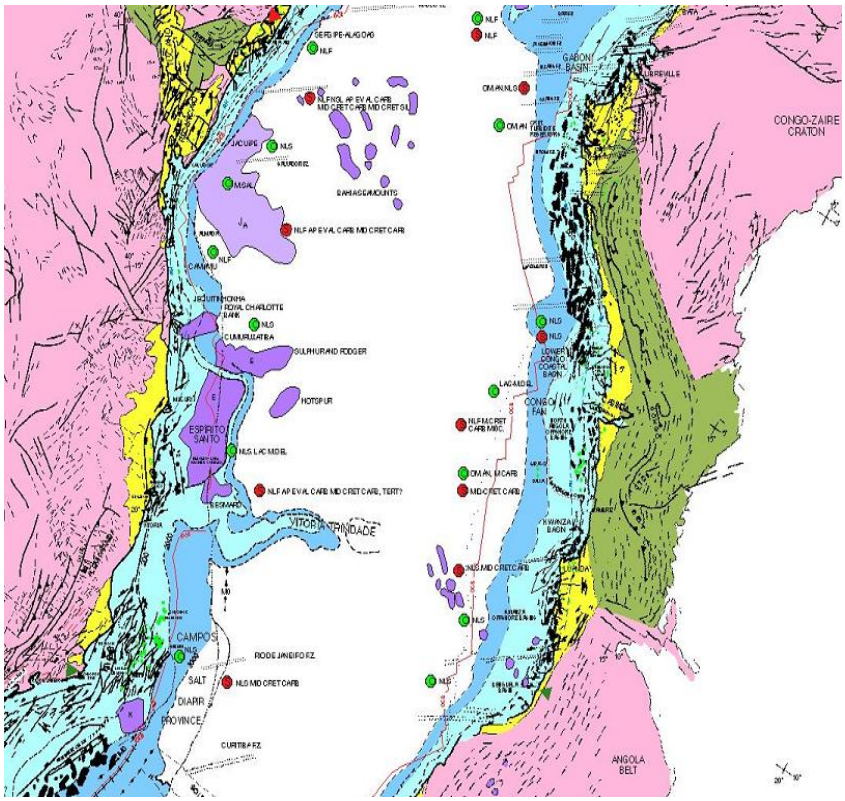

Figure 5.4.
The tectonic settings of the Angola and Brazilian margins (Davison, 1999).

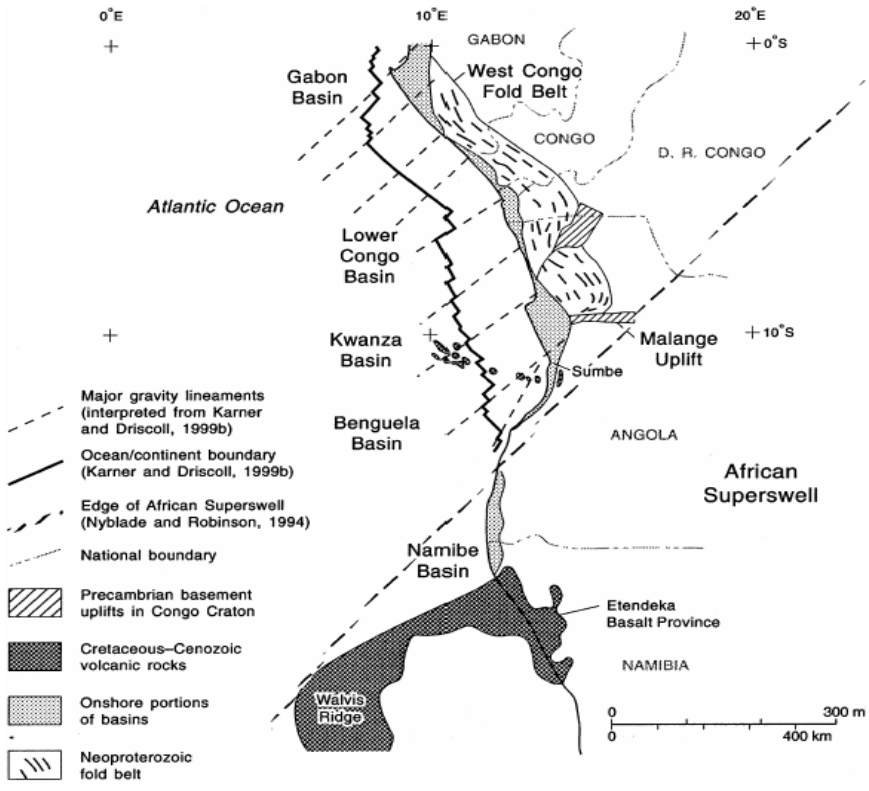

Figure 5.5.
Tectonic setting of the Lower Congo Basin, the Kwanza Basin and the Benguela Basin, Angola onshore/offshore (Hudec & Jackson, 2002).

Meyers et al. (1996) indicated the existence of non-volcanic slivers of uplifted mantle rocks in the Gabon Basin, associated with volcanic-rich zones. They also described the mechanism of the final rupture as developed above the thinnest portion of stretched and reheated lithosphere,

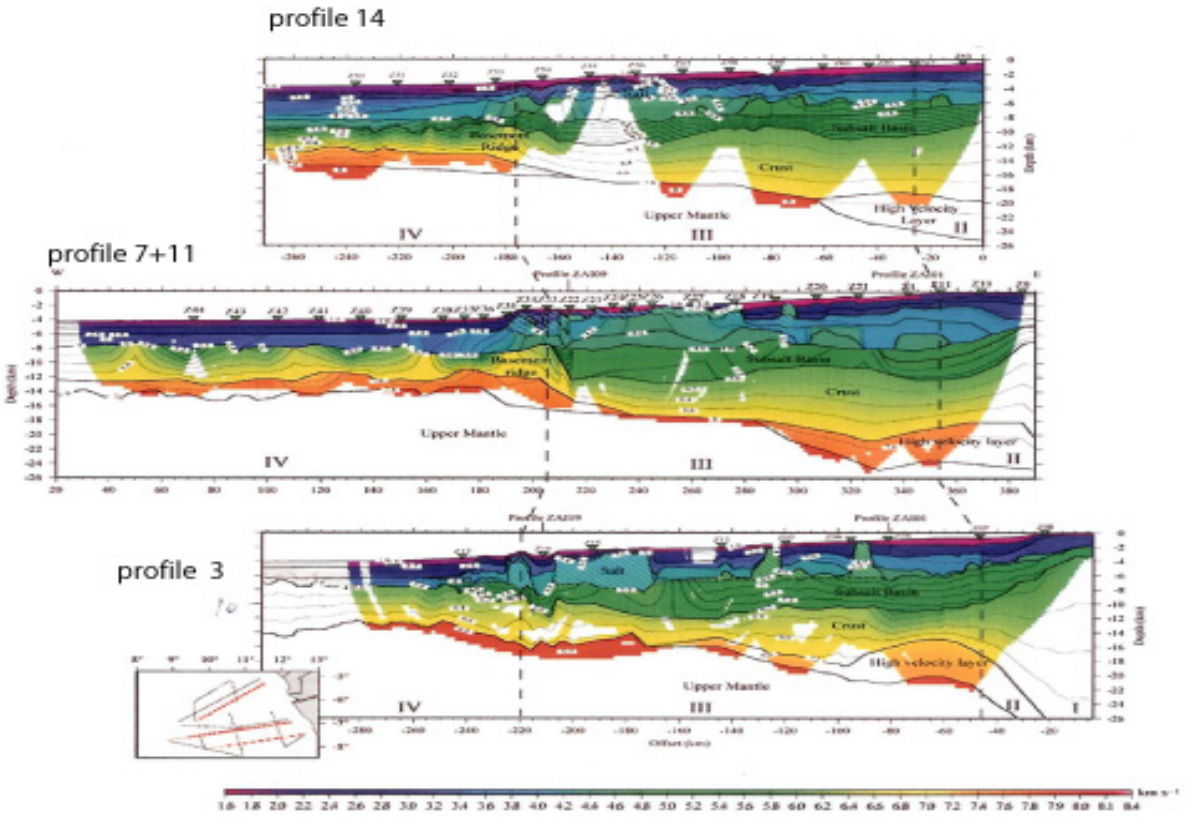

Figure 5.6. The profiles 14, 7+11 and 3 from Contrucci et al. (2004).

where decoupling occurred along weaknesses in the crust and upper mantle and basaltic melt intrudes along fault zones, sometimes isolating continental slivers. The erosion indicating the final breakup, has been postulated to occur as a consequence of buoyant uplift from underlying partial melt and/or redistributed flank uplift as the deep axis of the rift is flexed upward at the time of continental rupture.

Contrucci et al. (2004) and Moulin et al. (2005) provided the studies in the area located within the northern segment of this work (Fig. 5.6). The authors defined this area as non-volcanic and dismissed the assumption of underplating. However they did not accept the hypothesis of serpentinized mantle for the nature of LCB in this area either. On the sole basis of GM-SYS modelling it is not possible to discriminate between the two commonly proposed hypotheses. However, we note that the LCB is present within the segment with higher crustal thickness and within the vicinity of the onshore fold belt. That may give more points to the hypothesis of serpentinised mantle. At the same time the fact that the branches of the Kwanza volcanic line stretch inside the northern segment, cross Line B and probably reach Line A (Fig. 3.7) cannot be neglected and may indicate magmatism within the northern part of the study area.

The magmatism could have taken place in the northern part but in much lesser volume than in the southern part.

Significant lateral differences in the subsidence and structure of segments along extensional margins have been observed in various regions of the world. Campos and Santos Basins in Brazil are some of the examples. It was suggested that boundaries of the segments are deep transfer zones which remained active throughout the extensional phase of the margin. The transfer zones are deep faults, which dissect the margin perpendicular to the general strike into discrete segments. Segments exhibit distinct tectonic variations such as changes in the throw of normal faults and alternation of basement highs and lows along the margin. The presence of transfer zones within the Angolan margin was indicated by differences in the subsidence of these segments, revealed by burial history curves, and it was shown that the margin segments behaved tectonically independently, at least during their post-salt history (Spathopoulos, 1996).

It was also suggested (Spathopoulos, 1996; Rumph et al. 1993) that changes in the regional stress regime, in case of the West African margin, may have been caused by a change in the pole of rotation of the opening South Atlantic. It is also noted that differential subsidence across the fracture zones has focused sedimentation which resulted in location of the deltaic depocentres between fracture zones (Meyers et al., 1996; Reyer, 1984; Teisserenc & Villemin, 1989). The limits of crustal zones and faults appear to be offset across transfer zones, indicating compartmentalized extension within units bounded by transfer zones.

Within the study area, particular its southern part, several transfer zones were defined that cut the offshore area oblique to the coastline and die out landward within the onshore basins (Hudec & Jackson, 2002) (Figures 5.7 and 5.8). The boundary between the two segments of the study area coincides with the Luanda Transfer Zone. The boundary between the two provinces of the northern segment is also coincident with a transfer zone. Several authors point to the segmentation of the Angola margin by the strike-perpendicular transfer zones (Hudec & Jackson, 2002; Figueiredo & Murthy, 2002). Several features change across the transfer zones including basement geometry, salt related structural style, and sedimentation patterns (Fig. 4.7). The shear deformation along the transfer zones is evidenced by the geometries of the coastline, which stretches mostly along the margin and makes abrupt turns along the transfer zones. The valleys of the main rivers stretch in the direction of the transfer

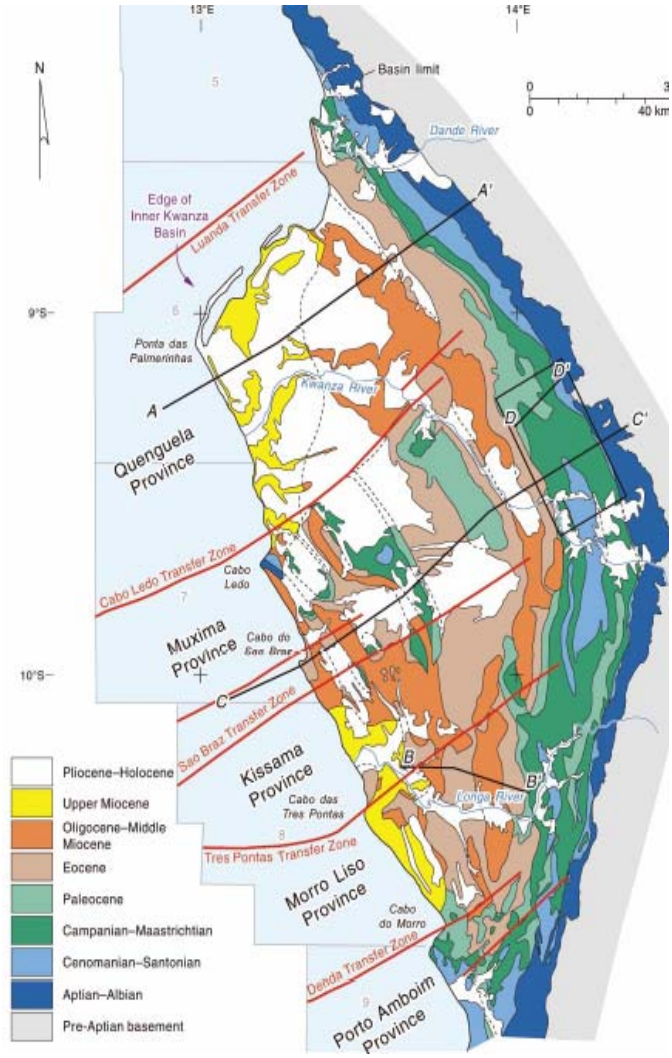

Figure 5.7. Geologic map of the Inner Kwanza Basin, Angola, showing approximate location of rift-related transfer zones (red) (Hudec & Jackson, 2002).

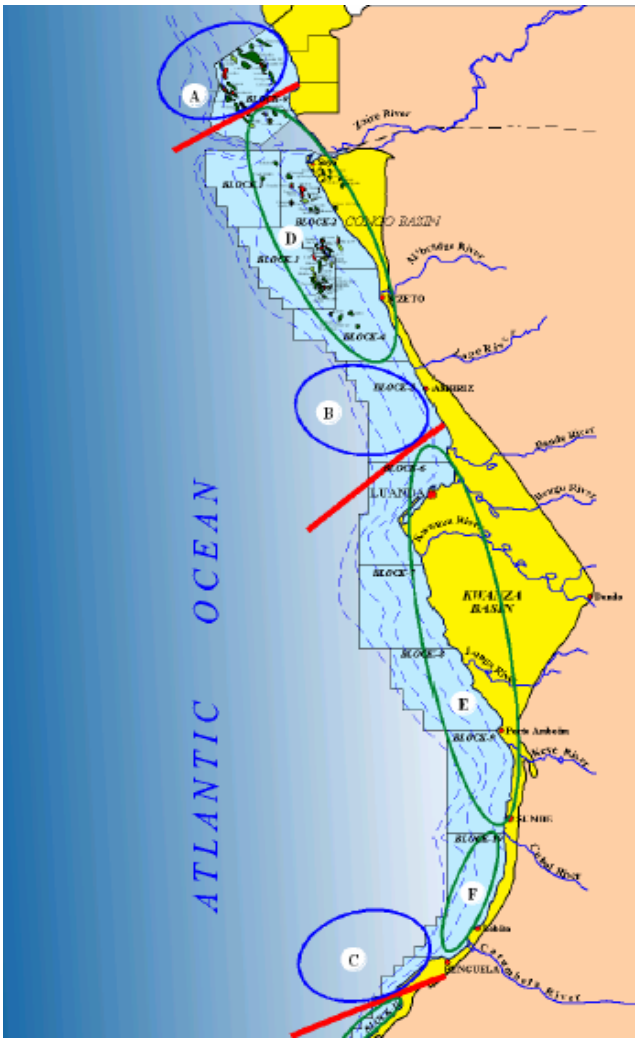

Figure 5.8. Angola Shelf margin showing Albian Siliclastic-Carbonate zones of deposition (Figueiredo & Murthy, 2002). Blue circles – siliclastic depocentres, green circles – carbonate shoal margin.

zones to almost 200 km inside the mainland, and can be attributed to weak fault zones that stretch in the direction of transfer zones onshore Angola. The Congo River stretches almost to 1000 km inside the continent subparallel to the direction of the transfer zone.

5.4 Brazilian and Angola conjugate margins

The conjugate margins of Brazil and West Africa carry on the similarities originated in the pre-breakup geological history of the margins. Davison (1999) indicated that sedimentary strata of Late Jurassic age are found on both sides of the Atlantic within the conjugate parts of the two margins. These sediments, consisting of coarse-grained fluvial sandstones, are

considered to have filled the Afro-Brazilian Depression that existed before the South Atlantic breakup. Hudec & Jackson (2002) [with reference to Cramez et al. (2000) and Cobbol et al. (2001)] noted that similar contractional features are related to folds, faults and uplifted mountain ranges that can be found on both conjugate margins. It was also argued that rift-related transfer zones linked to oceanic fractures were reactivated during the deformation leading to creation of similar structures (Hudec & Jackson, 2002). A number of unconformities that bound the rift sequences within the basins are found to be identical on both conjugate margins, increasing the number of similarities. Furthermore, rift architecture of the both margins is controlled by the two hinge zones, onshore and offshore the margins. The evaporites are late syn-rift deposits and are present on both margins (Karner & Driscoll, 1999). The post-rift development has also similarities. The sedimentation within the conjugate margins in the post-rift period was dominated by carbonate deposition. Furthermore, there are several similarities in the drainage system, such as that the direction of the main rivers close to the coastline is parallel to transfer zones on both sides from the Atlantic Ocean.

Dickson et al. (2003) in a large-scale reconstruction reprojected the continents and associated data for a range of ages. The reconstruction emphasized the zipper-like continental separation matching wide basins on one side with opposing narrow basins. The zipper-like pattern of separation produced the trend of juxtaposition of the wide sedimentary basin on one margin and narrow sedimentary basins or absence of any basin on the opposite margin. On Figure 5.4 the yellow colour stands for the sedimentary basins. Simple joining of the two sides exibits this trend.

The counterpart of the study area on the Brazilian side can be found by simple tracing of the fracture zones connected with the transfer zones (Fig. 5.10). The possibility for transfer zones to be connected to oceanic fracture zones has been extensively indicated (Hudec & Jackson, 2002; Figueiredo & Murthy, 2002; Mohriak & Rosendahl, 2002). Transfer zones within the Angola margin can be traced along fracture zones across the South Atlantic Ocean to the Brazilian margin on the bathymetry and gravity anomaly maps by distinctive linear features (Fig. 5.9). Simple tracing of the Hot Spur fracture zone on the Tectonic summary map of the South Atlantic from Davidson (1999) (Fig. 5.10) towards the African margin brings it to the north of the Kwanza Basin thus suggesting the Luanda Transfer Zone to be a continuation of

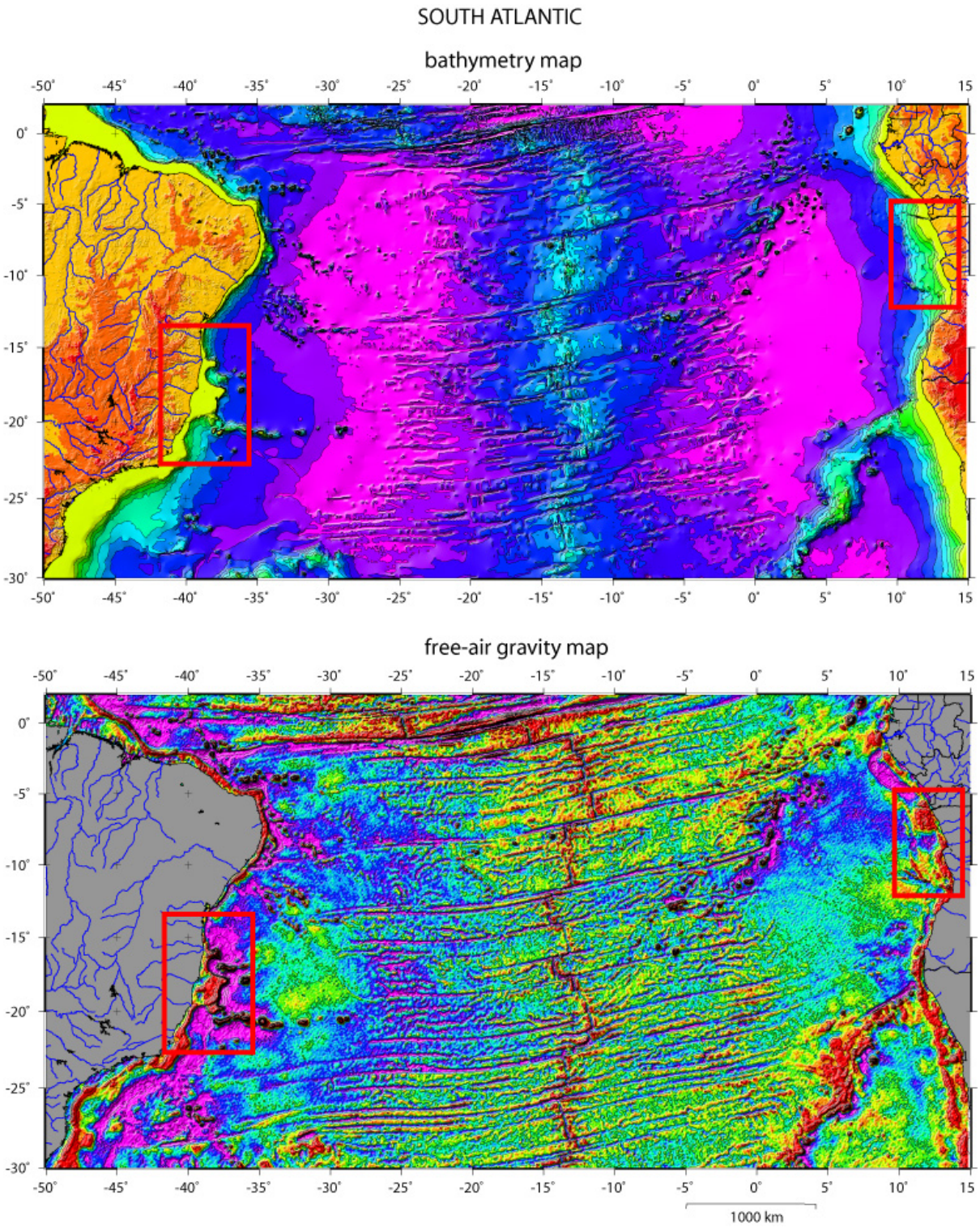

Figure 5.9. Bathymetry and free-air gravity anomaly maps for the South Atlantic. Location of study area off Angola and its conjugate on the Brazilian margin are shown by red box.

the Hot Spur Fracture Zone. The continuation of the St. Helena Fracture Zone crosses the northern border of the study area. The Bode Verde Fracture Zone can be traced towards the

Congo Basin. Tracing of these fracture zones to the opposite side of the South Atlantic defines the area conjugate to the study area. It is possible to note that the above named fracture zones, continued towards the Brazilian margin, slightly separate, thus embracing larger area on the Brazilian side than on African side. As it was mentioned in the chapter Geological Framework, movement of the two continents was associated with the clock-wise rotation of one plate relatively to the other. The larger conjugate area on Brazilian margin may suggest that rotation included deformation of the Brazilian plate, particularly extension within the plate. Reconstruction of the South Atlantic region for different ages was also made by Macdonald et al. (2002) (Figures 2.1 and 2.2). According to this reconstruction the wide area on the Brazilian margin where the Camamu Basin, the Espirito Santo Basin and the Campos Basin are located is conjugate to a narrower area on the African margin with the Congo Basin and the Kwanza Basin (Fig. 5.11).

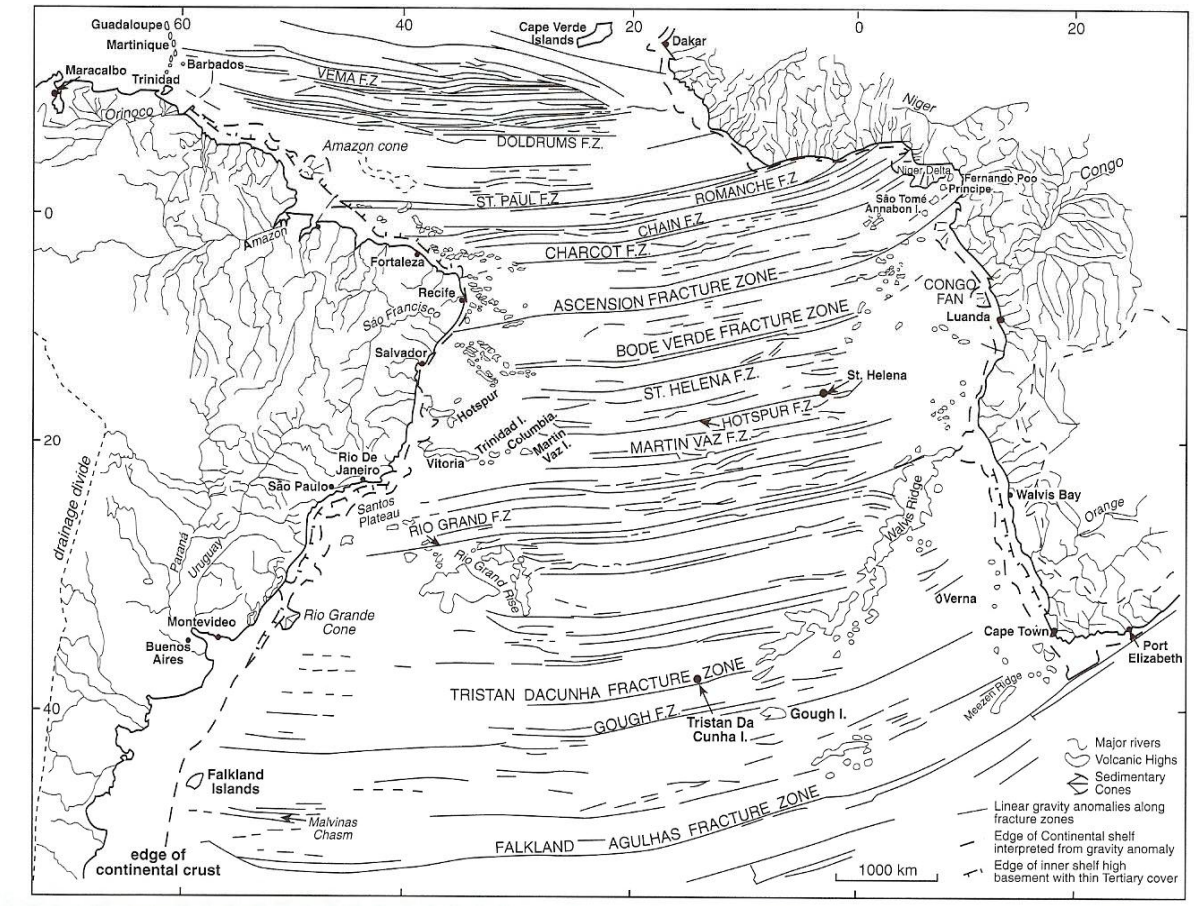

Figure 5.10. Tectonic summary map of the South Atlantic (Davison, 1999).

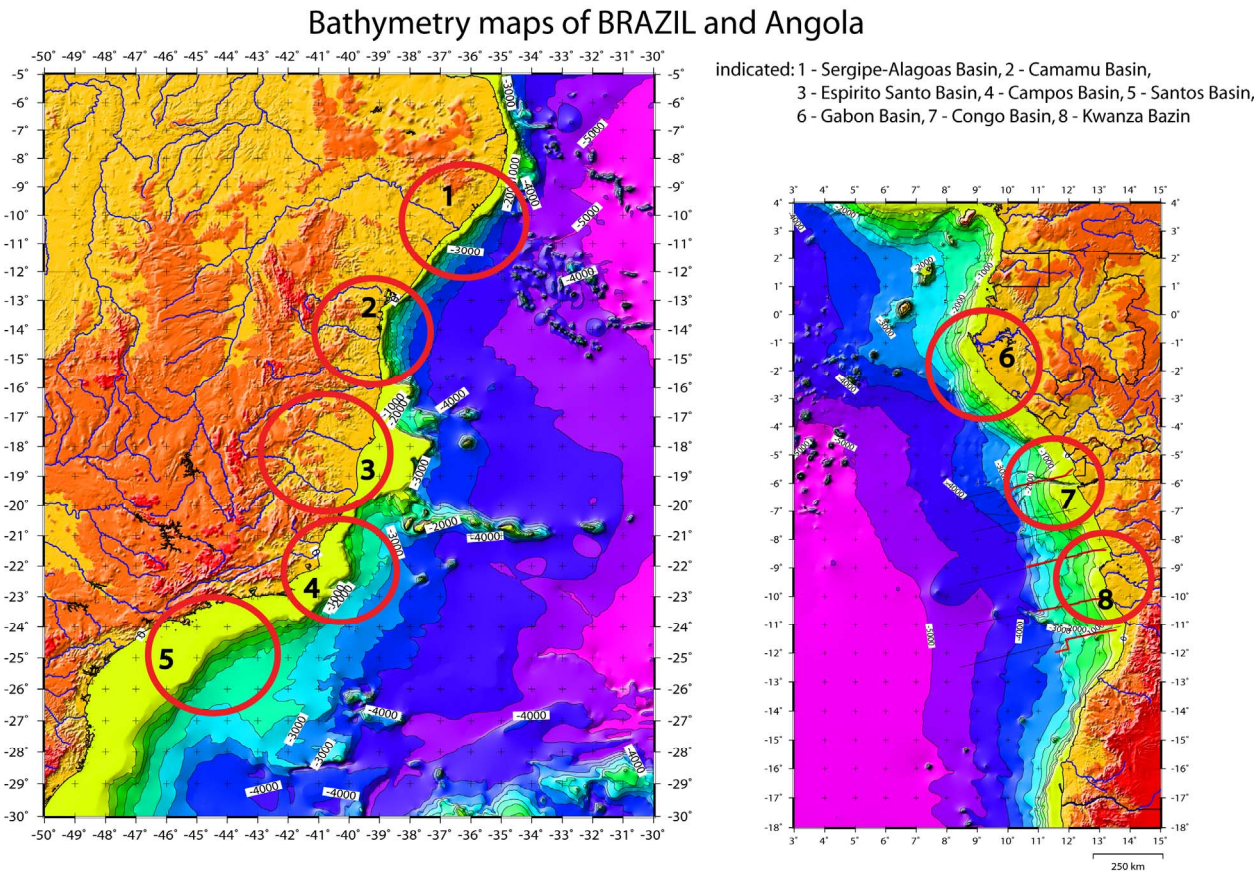

Figure 5.11. The sedimentary basins on the conjugate margins off Brazil and Angola.

6. SUMMARY AND CONCLUSIONS

Based on integrated analysis of seismic reflection and potential field data and 2D gravity modelling the crustal structure offshore Angola was studied. The analysis revealed a framework of margin segmentation within the study area. In particular, the northern segment, to which the Lower Congo Basin belongs, exhibits overall low-amplitude gravity anomalies, while the southern segment, where the Kwanza Basin and the Benguela Basin are located, exhibits significantly higher amplitude gravity anomalies. The difference in overall gravity values was attributed to the different thickness of the crust within the segments. 2D gravity modelling has shown that the relatively thicker crust is a characteristic feature of the northern segment, while within the southern segment the crust is considerably thinner except the parts where the crust is overprinted by magmatism.

The continental crust within the study area exhibits a non-uniform structure. When in Line A the average crustal density within the continental domain has values of 2.8 g/cm^3, to the south of this line, particular in lines B and C, the crustal density values change from 2.85 g/cm^3 to 2.8 g/cm^3 landward.

The continent-ocean boundary/transition (COB/COT), delineated close to the prominent positive-negative gradient on Bouguer anomalies, exhibits the imprint of both extension and shear motion as the two main types of deformation that the Angola margin has undergone.

A high seismic velocity and density Lower Crustal Body was defined within the northern margin segment. Even if the definition of the nature of the LCB is beyond the scope of this work, the body is most likely related to high-grade metamorphic rocks.

The magmatism has significantly overprinted the southern segment. The northern segment was not affected by magmatism at the same rates as the southern segment; however the magmatism could have taken place within the northern segment as the 2D gravity modelling has shown that the northward stretching branches of the Kwanza volcanic line have built the highs on the top basement level within lines B and C.

Mapping of the fracture zones within the study area reveals a framework of structural inheritance and has shown that the fracture zones can be traced towards the continent where

they continue as transfer zones. The boundary between the northern and southern segments was considered to be coincident with the Luanda Transfer Zone which in its turn was considered to be a continuation of the Hot Spur Fracture Zone. The segment boundary continues toward the continent and separates the mainland into a lowland and a highland region.

Simple tracing of the fracture zones across the Atlantic Ocean helped to define the conjugate counterpart for the study area. The fact that the counterpart on the Brazilian side is slightly wider, may be attributed to extension within the continent associated with clock-wise rotation of the Brazilian plate relative to the African plate. Furthermore, comparison of the basins on the conjugate margins revealed the trend of juxtaposition of wide sedimentary basins in one margin and narrow sedimentary basins at the conjugate margin. This asymmetry in the margins architecture is consistent with the zipper-like continental separation noticed by several other studies in the region.

REFERENCES

Contrucci L., Matias L., Moulin M., Geli L., Klingelhofer, Nouze H. et al., 2004. Deep structure of the West African continental margin (Congo, Zair, Angola), between 5°S and 8°S, from reflection/refraction seismic and gravity data. *Geophys. J. Int., 158, 529-553.*

Cramez C., Jackson M.P.A., 2000. Superposed deformation straddling the continental-oceanic transition in deep-water Angola. *Marine and Petroleum Geology, 17 (2000) 1095-1109.*

Davison I., 1999. Tectonic and hydrocarbon distribution along the Brazilian South Atlantic margin. *Geological Society Special Publication, 153.*

Dickson W.G., Fryklund R.E., Odegard M.E., Green C.M., 2003. Constrains for plate reconstruction using gravity data – implications for source and reservoir distribution in Brazilian and West African margin basins. *Marine and Petroleum Geology, 20 (2003) 309-322.*

Figueiredo C., Murthy I., 2002. Pinda Reservoirs and Prospectivity. *AAPG Annual Meeting, March 10-13, 2002.*

Gjelberg John G., Valle Paul J., 2003. Tectonostratigraphic evolution of the offshore Angolan margin. *Norsk Hydro, Bergen.*

Gladczenko T. P., Skogseid J., Eldholm O., 1998. Namibia volcanic margin. *Marine Geophysical Researches, 20, 313-341*.

Hudec M., Jackson M., 2002. Structural segmentation, inversion, and salt tectonics on a passive margin: Evolution of the Inner Kwanza Basin, Angola. *GSA Bulletin, October 2002, p. 1222-1244.*

Hudec M., Jackson M., 2004. Regional restoration across the Kwanza Basin, Angola: Salt tectonics triggered by repeated uplift of a metastable passive margin. *AAPG Bulletin, v.88, No. 7, pp. 971-990.*

Karner G.D., Driscoll N., 1999. Tectonic and stratigraphic development of the West African and Eastern Brazilian Margins: insight from quantitative basin modelling. *Geological Society, Special Publications, 153, 11-40.*

Macdonald D., Gomez-Perez I., Franzeze J., Spaletti L. et al., 2002. Mesozioc break-up of SW Gondwana: implications for regional hydrocarbon potential of the southern South Atlantic. *Marine Petroleum Geology, 20, 287-308.*

Marton L. G., Tari G. C., Lehmann C. T., 2000. Evolution of the Angolan Passive Margin, West Africa, with Emphasis on Post-Salt Structural Styles. Atlantic Rifts and Continental Margins. *Geophysical Monograph, 115.*

Meyers J. B., Rosendahl B. B., Austin J. A., 1996. Deep-penetrating MCS images of the South Gabon Basin: implications for rift tectonics and post-breakup salt remobilization. *Basin Research, 8, 65-84.*

Mohriak W.U., Rosendahl B.R., 2002. Magmatic activity, Fracture Zones and their relationship to the origin and evolution of the South Atlantic: Crustal Architecture and Tectonic Evolution of conjugate sedimentary basins from Gabon to Namibia. *AAPG Hedberg Conference "Hydrocarbon Habitat of Volcanic rifted Passive Margins", September 8-11, 2002, Stavanger, Norway*.

Moulin M., Aslanian D., Olivet J.-L., Contrucci I., Matias L. et al., 2005. Geological constrains on the evolution of the Angolan margin based on the reflection and refraction seismic data (ZaiAngo project). *Geophys. J. Int., 162, 793-810.*

Schiefelbein C.F., Zumberge J.E.; Cameron N.C., Brown S.W., 2000. Geochemical copmparison of crude oil along the South Atlantic margins. *AAPG Memoir 73, p.15-26.*

Spathopoulos F., 1996. An insight on salt tectonics in the Angola Basin, South Atlantic. *Geological Society Special Publications, 100, 153-174.*

Stewart J., Watts A. B., Bagguley J. G., 2000. Three-dimensional subsidence analysis and gravity modelling of the continental margin offshore Namibia. *Geophys. J. Int., (2000) 141, 724-746.*

Valle Paul J., Gjelberg John G., Helland-Hansen W., 2001. Tectonostratigraphic development in the eastern Lower Congo Basin, offshore Angola, West Africa. *University of Bergen, Norsk Hydro, Bergen.*

Valle Paul J., Sperrevik S., Gjelberg J. G., 2003. Structural impact on deep-marine sedimentary systems in The Lower Congo Basin, offshore Angola. Part 1: Seismic analysis. Interplay between Deep-Marine Sedimentary Systems and Salt Tectonics Offshore Angola, West Africa, Ch.4.

Watts A.B., Stewart J., 1998. Gravity anomalies and the segmentation of the continental margin offshore West Africa, *Earth planet. Sci. Lett., 156, 239-252.*

Web-site http://www.ngdc.noaa.gov/mgg/gebco/gebco.html

Web-site http://www.ngdc.noaa.gov/mgg/sedthick/sedthick.html

Web-site http://www.npagroup.co.uk/oilandmineral/onshore/studies/region_satlantic.htm